Available online at www.sciencedirect.com
ScienceDirect
Geochimica et Cosmochimica Acta 73 (2009) 3864–3879
Geochimica et Cosmochimica Acta
www.elsevier.com/locate/gca

Elucidating microbial processes in nitrate- and sulfate-reducing systems using sulfur and oxygen isotope ratios: The example of oil reservoir souring control

Casey Hubert [a,*], Gerrit Voordouw [a], Bernhard Mayer [b]

[a] Department of Biological Sciences, University of Calgary, 2500 University Drive NW, Calgary, Alta., Canada T2N 1N4
[b] Department of Geoscience, University of Calgary, 2500 University Drive NW, Calgary, Alta., Canada T2N 1N4

Received 5 February 2008; accepted in revised form 17 March 2009; available online 1 April 2009

Abstract

Sulfate-reducing bacteria (SRB) are ubiquitous in anoxic environments where they couple the oxidation of organic compounds to the production of hydrogen sulfide. This can be problematic for various industries including oil production where reservoir "souring" (the generation of H_2S) requires corrective actions. Nitrate or nitrite injection into sour oil fields can promote SRB control by stimulating organotrophic nitrate- or nitrite-reducing bacteria (O-NRB) that out-compete SRB for electron donors (biocompetitive exclusion), and/or by lithotrophic nitrate- or nitrite-reducing sulfide oxidizing bacteria (NR-SOB) that remove H_2S directly. Sulfur and oxygen isotope ratios of sulfide and sulfate were monitored in batch cultures and sulfidic bioreactors to evaluate mitigation of SRB activities by nitrate or nitrite injection. Sulfate reduction in batch cultures of *Desulfovibrio* sp. strain Lac15 indicated typical Rayleigh-type fractionation of sulfur isotopes during bacterial sulfate reduction (BSR) with lactate, whereas oxygen isotope ratios in unreacted sulfate remained constant. Sulfur isotope fractionation in batch cultures of the NR-SOB *Thiomicrospira* sp. strain CVO was minimal during the oxidation of sulfide to sulfate, which had $\delta^{18}O_{SO4}$ values similar to that of the water–oxygen. Treating an up-flow bioreactor with increasing doses of nitrate to eliminate sulfide resulted in changes in sulfur isotope ratios of sulfate and sulfide but very little variation in oxygen isotope ratios of sulfate. These observations were similar to results obtained from SRB-only, but different from those of NR-SOB-only pure culture control experiments. This suggests that biocompetitive exclusion of SRB took place in the nitrate-injected bioreactor. In two replicate bioreactors treated with nitrite, less pronounced sulfur isotope fractionation and a slight decrease in $\delta^{18}O_{SO4}$ were observed. This indicated that NR-SOB played a minor role during dosing with low nitrite and that biocompetitive exclusion was the major process. The results demonstrate that stable isotope data can contribute unique information for understanding complex microbial processes in nitrate- and sulfate-reducing systems, and offer important information for the management of H_2S problems in oil reservoirs and elsewhere.

1. INTRODUCTION

1.1. Anaerobic carbon, sulfur and nitrogen cycling

Environments containing organic matter under anaerobic conditions are home to diverse microbial communities. Sulfate- and nitrate-reducing microorganisms in these habitats may use similar organic electron donors as carbon and energy sources. In natural settings such as aquatic sediments biogeochemical processes are oriented according to the redox potentials of electron acceptors such that nitrate reduction oxidizes organic substrates earlier and more efficiently than bacterial sulfate reduction (Jørgensen, 2006). Nitrate- and sulfate-reducing zones can also come into contact due to wind mixing, upwelling or eutrophication (Naqvi et al., 2000; Dale et al., 2009). Hydrogen sulfide produced

* Corresponding author. Present address: Max Planck Institute for Marine Microbiology, Celsiusstraβe 1, 28359-Bremen, Germany. Fax: +49 421 2028 690.
E-mail address: chubert@mpi-bremen.de (C. Hubert).

0016-7037/$ - see front matter © 2009 Elsevier Ltd. All rights reserved.
doi:10.1016/j.gca.2009.03.025

by sulfate-reducing bacteria (SRB) can also serve as an electron donor for nitrate-reduction. The products of nitrate-reduction include nitrite, which can inhibit sulfate reducers, but which also serves as an electron acceptor for the oxidation of organic or reduced sulfur-containing electron donors. Hence in anoxic environments the biogeochemical carbon, nitrogen and sulfur cycles are intimately intertwined, yet there is still a lack of basic understanding of some of the complex interdependencies at the microbial level. There is also a significant applied interest in the outcome of these interactions, as the microbial processes may have beneficial or detrimental consequences for different industries (e.g., wastewater treatment, petroleum production) where responsible management depends on a sound understanding of the relevant microbial ecology. One example is the petroleum industry where souring of reservoirs by microbial H_2S production causes significant operational problems.

1.2. The example of oil reservoir souring control using nitrate and nitrite

Effective containment of oil reservoir souring can be achieved by incorporating nitrate or nitrite injection into water flooding regimes during secondary oil production to stimulate nitrate- or nitrite-reducing bacteria (NRB; Hubert et al., 2005). Microbiological strategies for the control of oil field souring have been investigated in recent years by cultivating pure and mixed cultures of oil field microbes, and using molecular approaches such as 16S rRNA gene cloning, reverse sample genome probing, denaturing gradient gel electrophoresis and fluorescence *in situ* hybridization to monitor oil field microbial community shifts following nitrate or nitrite treatment (Voordouw et al., 1996; Telang et al., 1997; Gevertz et al., 2000; Eckford and Fedorak, 2002; Hubert et al., 2003; Kjellerup et al., 2005; Bødtker et al., 2008; Grigoryan et al., 2008; Jurelevicius et al., 2008; Schwermer et al., 2008). Manipulating the microbial community so that sulfide gets eliminated depends on interactions between SRB and NRB in oil reservoirs. Organotrophic NRB (O-NRB) can oxidize oil-derived organic compounds that serve as electron donors for microbial growth. Depletion of such compounds by O-NRB can prevent bacterial (dissimilatory) sulfate reduction (BSR) that is supported by the same electron donors (Fig. 1a). This is referred to as biocompetitive exclusion, and results in souring control. Lithotrophic nitrate- or nitrite-reducing sulfide-oxidizing bacteria (NR-SOB) can also control souring by directly consuming sulfide as their electron donor for microbial growth (Fig. 1b).

Careful examination of Fig. 1 reveals that both scenarios mediate the overall oxidation of oil organics with nitrate, catalyzed directly by O-NRB or indirectly via sulfur cycling between NR-SOB and SRB. Hence, chemical concentration profiles of the reactants and products depicted schematically in Fig. 1 cannot conclusively determine which souring control mechanism is operating in a given environment (Hubert et al., 2003). Molecular approaches that rely on gene sequences from relevant microbes can be useful in determining which process may be occurring. However,

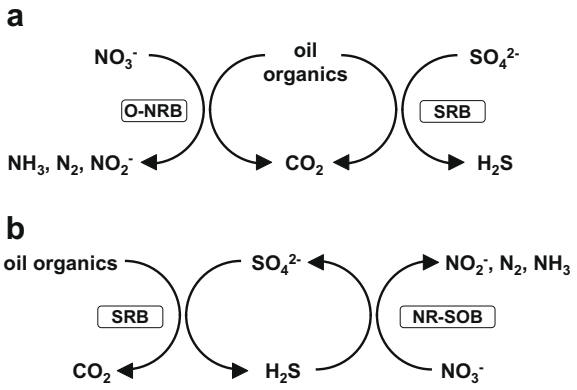

Fig. 1. The impact of nitrate or nitrite on the activity of SRB. (a) O-NRB compete directly with SRB for organic electron donors, resulting in the biocompetitive exclusion of the SRB. (b) Sulfide produced by SRB can be recycled back to sulfate via nitrate reduction by lithotrophic NR-SOB. In either mechanism nitrite can be substituted for nitrate as the electron acceptor for NRB.

molecular techniques can be inconclusive, e.g., in cases where the nitrate reducers responsible for oil reservoir souring control are facultative chemolithotrophs such as *Sulfurospirillum* spp. that can oxidize both sulfide and organic compounds with nitrate (Hubert and Voordouw, 2007). Additional tools are thus required to more conclusively elucidate which combinations of reaction pathways are responsible for sulfide removal in oil reservoirs and other anoxic environments.

While this work was motivated by oil reservoir souring scenarios, our findings extend and apply to other industrial and natural settings. We have retained the terms "souring" and "souring control" throughout this article, which are interpreted broadly to refer to other industrial contexts where sulfide is problematic and to natural environments where nitrate or nitrite reduction can offset the accumulation of sulfide produced by SRB.

1.3. Stable isotope approaches for elucidating redox reactions in the sulfur cycle

Stable isotope ratio measurements are being used increasingly to reveal the sources and fates of compounds in microbial reaction pathways (Fry, 2006). It is well known that the light isotope ^{32}S is metabolized preferentially during BSR (e.g., Harrison and Thode, 1958; Mizutani and Rafter, 1969) due to isotope effects associated with individual steps in the dissimilatory sulfate reduction pathway (Rees, 1973). As the light isotope ^{32}S is metabolized more rapidly during BSR, the remaining sulfate becomes progressively enriched in ^{34}S as the sulfate concentration decreases. In a closed system this can be described by the Rayleigh equation:

$$R_t/R_0 = (C_t/C_0)^{[(1/\alpha)-1]} \quad (1)$$

R_t and R_0 denote S isotope ratios of sulfate, C_t and C_0 represent the fraction (f) of the sulfate concentrations at times t and zero, respectively, and α is the isotope fractionation

factor. In aquatic environments sulfur isotope fractionation factors associated with BSR are typically 1.010–1.020 (e.g., Strebel et al., 1990) and can be converted to an isotope enrichment factor (ϵ) as follows:

$$\epsilon = (\alpha - 1) \times 10^3 \quad (2)$$

Isotope enrichment factors during BSR are thus often 10–20‰. If the difference between R_t and R_0 is small, the Rayleigh equation can be simplified to:

$$R_t = R_0 \times f^{(\alpha-1)} \quad (3)$$

where f is the fraction of remaining sulfate (Clark and Fritz, 1997) and thus effectively represents the inverse of the extent of BSR. Isotope ratios of sulfide and sulfate (expressed as δ values) can be plotted against the natural logarithm of f to determine the isotope enrichment factor during BSR (Bolliger et al., 2001). Rayleigh fractionation expressed with negative values indicates enrichment of the light isotope ^{32}S in the produced sulfide. Overall isotope fractionation during BSR can vary from less than −10‰ to more than −49‰ depending on environmental factors such as sulfate concentration (Harrison and Thode, 1957; Kaplan and Rittenberg, 1964), the availability and type of carbon source (Canfield, 2001; Detmers et al., 2001), temperature (Canfield et al., 2006), cell specific sulfate reduction rates (Detmers et al., 2001) and the degree to which cell-internal intermediates are reoxidized (Mangalo et al., 2007). In a closed experimental system where sulfate is not limiting, the $\delta^{34}S_{H2S}$ of the produced sulfide is initially significantly lower than that of the sulfate. As BSR proceeds and f decreases from 1 to 0 the $\delta^{34}S_{H_2S}$ progressively increases, finally returning to the value of the original sulfate once BSR is complete ($f = 0$).

Oxygen isotope effects during BSR have been studied in less detail than S isotope fractionation. Initial studies suggested that $\delta^{34}S_{SO_4}$ and $\delta^{18}O_{SO_4}$ in remaining sulfate both increase, often at a ratio of approximately 4:1 (Mizutani and Rafter; 1969). More recent research, however, has shown that $\delta^{34}S_{SO_4}$ can approach a constant value, while $\delta^{34}S_{SO_4}$ values continue to increase (Mizutani and Rafter, 1973; Fritz et al., 1989; Aharon and Fu, 2000, 2003; Böttcher et al., 2001). During BSR, $\delta^{18}O_{SO_4}$ may be influenced by equilibrium oxygen isotope exchange between water and adenosine phosphosulfate or sulfite, which is followed by back-reactions that ultimately influence the $\delta^{18}O_{SO_4}$ of sulfate remaining in solution (Mizutani and Rafter, 1973; Fritz et al., 1989; Spence et al., 2001; Brunner et al., 2005; Knoeller et al., 2006; Mangalo et al., 2007, 2008; Zopfi et al., 2008). Oxygen isotope ratios in unreacted sulfate during BSR may indeed depend on a combination of kinetic and equilibrium isotope effects (Wortmann et al., 2007).

Microbial oxidation of sulfide and other reduced sulfur compounds is generally associated with relatively small S isotope fractionation (Fry et al., 1986; Balci et al., 2007; De Gusseme et al., 2009; Zerkle et al., 2009), due in part to many such reactants (e.g., elemental sulfur and metal sulfides) existing as solids limiting the opportunity for isotopic discrimination. Under aerobic conditions O_2 and H_2O are both potential oxygen sources for newly formed sulfate (Van Stempvoort and Krouse 1994; Taylor and Wheeler 1994; Ku et al., 1999; Balci et al. 2007), whereas under anaerobic conditions (e.g., with dissolved ferric iron) all sulfate–oxygen is usually derived from water (Balci et al., 2007). Newly formed sulfate during sulfide oxidation generally has a $\delta^{18}O_{SO_4}$ below +5‰ and can be as low as −20‰, depending on the environmental conditions and the $\delta^{18}O_{H_2O}$ of ambient water (Van Stempvoort and Krouse, 1994; Balci et al., 2007). Oxygen isotope exchange between water and sulfate is extremely slow at near-neutral pH values and environmental temperatures (Lloyd, 1967; Zak et al., 1980; Chiba and Sakai, 1985). Therefore, once sulfate has formed via oxidation, its O isotope ratio is usually preserved.

Analyzing concentrations and isotopic compositions of sulfide and sulfate may hold potential for enhancing the understanding of microbial processes in anoxic systems that are characterized by sulfate-, nitrate- and nitrite-reducing conditions. For the present study, we hypothesized that if O-NRB compete with SRB for organic electron donors (Fig. 1a) then increasing nitrate or nitrite (NO_x) doses should result in progressive exclusion of SRB, hence a progressive decrease in BSR. This should result in Rayleigh-type sulfur isotope fractionation patterns in experimental bioreactors, with isotope ratios of sulfate progressing towards those of the initial sulfate as the extent of BSR declined (i.e., at higher NO_x doses as f increases from 0 to 1; see Section 4.2.1). Alternatively, if NR-SOB catalyze sulfide oxidation to sulfate, trends to lower sulfur and oxygen isotope ratios should result due to different sulfur isotope fractionation effects and incorporation of ^{18}O-depleted water–oxygen into the newly formed sulfate, respectively (see Section 4.3.1). With the above premise in mind, the objective of our study was to evaluate the usefulness of applying sulfur and oxygen isotope measurements for distinguishing between organotrophic and lithotrophic nitrate and nitrite reduction pathways in anoxic environments with SRB activity.

2. MATERIALS AND METHODS

Up-flow, packed-bed bioreactors were used to study BSR and sulfide oxidation in oil field simulations under nitrate- and nitrite-reducing conditions. Isotope patterns during BSR and sulfide oxidation were additionally evaluated in separate batch culture experiments.

2.1. Pure cultures of oil field NRB and SRB

The oil field sulfate-reducing *Desulfovibrio* sp. strain Lac15 (Voordouw et al., 1996) was maintained in saline Postgate C medium (sPGC; Telang et al., 1999) and subsequently inoculated (1% v/v) into 1-l experimental flasks (Fig. 2a) containing 800 ml of lactate- and sulfate-amended CSB-A medium (Table 1; Hubert et al., 2003) to study isotope effects during BSR. A model oil field NR-SOB, *Thiomicrospira* sp. strain CVO (Telang et al., 1997; Gevertz et al., 2000; Greene et al., 2003), was maintained in nitrate- and sulfide-amended CSB-A medium (Table 1). Fully grown cultures (100 ml) were used to harvest CVO cells by centrifugation inside an anaerobic hood. Washed cell

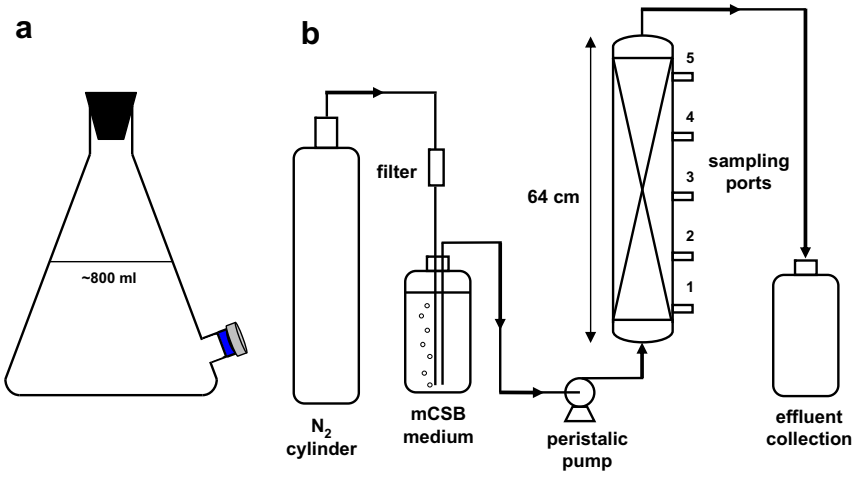

Fig. 2. Experimental set up for (a) batch culture and (b) up-flow packed-bed bioreactor experiments.

Table 1
Initial medium conditions for different experiments.

Parameter	SRB batch CSB-A[a]	NR-SOB batch CSB-A	NO_3^- treated bioreactor mCSB[b] + nitrate	NO_2^- treated bioreactors mCSB + nitrite
Sulfate	8 mM	0 mM	6 mM	8 mM
Lactate	25 mM	0 mM	12.5 mM	25 mM
Excess lactate[c]	9 mM	NA[d]	0.5 mM	9 mM
Sulfide	0 mM	6 mM	0 mM	0 mM
Nitrate	0 mM	30 mM	0–15 mM	0 mM
Nitrite	0 mM	0 mM	0 mM	0–20 mM
$\delta^{34}S_{SO_4}$	+4‰	NA	+6.1 ± 0.8‰	+6.1 ± 0.3‰
$\delta^{18}O_{SO_4}$	+11‰	NA	+7.9 ± 1.1‰	+10.0 ± 0.9‰
$\delta^{18}O_{H_2O}$	−18‰[e]	−18‰	−18‰	−18‰
$\delta^{34}S_{H_2S}$	NA	+1‰	NA	NA

[a] Coleville synthetic brine (Hubert et al., 2003).
[b] Modified coleville synthetic brine (Nemati et al., 2001).
[c] Lactate in excess of 2:1 ratio (lactate:sulfate) required for complete BSR (see Section 3.2.1).
[d] Not applicable.
[e] As demonstrated for Calgary tap water (Peng et al., 2004; Ferguson et al., 2007; see Section 2.3).

pellets representing 20–50% of the original cultures were resuspended in 1–2 ml of medium and inoculated into 1-l experimental flasks containing 500–800 ml of medium. Experimental flasks were sampled periodically from the side-arm port to evaluate isotope effects during BSR and sulfide oxidation. All CSB media were anoxic and bicarbonate-buffered (Hubert et al., 2003).

2.2. Bioreactor set-up

Three bioreactors were set up and operated as shown in Fig. 2b and described by Hubert et al. (2003). A glass column equipped with five sampling ports was packed with sand, autoclaved, filled with sterile anoxic modified Coleville synthetic brine (mCSB; bicarbonate-buffered medium containing lactate and sulfate for growth of SRB) and inoculated at each of five ports with 15 ml of produced water from the Coleville oil field in Saskatchewan, Canada (obtained in April 2002). This water is co-produced with oil and separated prior to oil transport and refining, making it a good source of microorganisms from oil field systems. Produced water was the only inoculum introduced to the bioreactors. Following batch-wise operation for ca. 1 month, flow rates were increased from 0 to 9 ml/h to allow development of an active SRB biofilm. This gave rise to a retention time of ca. 24 h when the flow rate was 9 ml/h (Hubert et al., 2003). Inflowing anoxic mCSB medium was then amended with nitrate (KNO_3, initially 2.5 mM) or nitrite ($NaNO_2$, initially 4 mM). Different media are summarized in Table 1. Concentrations of sulfide, sulfate, nitrate, nitrite, lactate and acetate, as well as the redox potential (E_h), were monitored. Once steady state conditions were established with respect to these parameters, nitrate or nitrite concentrations were increased in 2.5 or 4 mM increments, respectively. Steady state conditions were indicated by constant chemical profiles for 3 consecutive days, which usually required a total of 8–11 days operation at each nitrate or nitrite dose. Once parallel nitrite

treatments (two bioreactors) both reached steady state conditions with 20 mM, one of the nitrite-treated bioreactors was stopped (bioreactor A) while the other operated for an additional 60 days with 20 mM nitrite addition (bioreactor B).

2.3. Analytical procedures

Sulfide concentration was determined spectrophotometrically (Cord-Ruwisch, 1985). Sulfate concentration was determined spectrophotometrically (Nemati et al., 2001) and using a Waters 600E high-pressure liquid chromatograph (HPLC) with a Waters 423 conductivity detector, using a Waters IC-Pak HC column and a borate/gluconate eluent (Waters) at 2 ml min^{-1}. Nitrate and nitrite concentrations were determined using the same Waters 600E HPLC equipped with a Gilson Holochrome UV detector at 200 nm. Some nitrite concentrations were determined spectrophotometrically (APHA, 1992). The alternative approaches for measuring sulfate and nitrite concentrations were in good agreement. Lactate and acetate concentrations were determined using a Waters 600E HPLC equipped with a Waters 2487 UV detector at 220 nm, using an Alltech Prevail Organic Acid column (250 × 4.6 mm) and 25 mM KH_2PO_4 (pH 2.4) as the eluent at 1 ml min^{-1}. Redox potential differences, ΔE_h, were measured offline using a microelectrode and an Ag/AgCl reference electrode ($E_h = +222$ mV) from Microelectrodes Inc. (Bedford, NH, USA). E_h was calculated as $E_h = \Delta E_h + 222$. The electrode was calibrated with an ORP standard solution (Orion Research Inc., Beverley, MA) with $\Delta E_h = +424$ mV at 20 °C.

Isotopic compositions of sulfide and sulfate were also determined. Batch cultures were sampled with a syringe and aliquots were introduced directly into cadmium acetate solution to halt microbial activity and precipitate any sulfides present as cadmium sulfide. Bioreactor liquid was sampled from inflowing medium via diversion tubing and from bioreactor sampling ports using syringes. Cadmium sulfide precipitate was removed by filtration, converted to Ag_2S and dried for further analyses. The remaining sulfate in solution was precipitated as $BaSO_4$ via addition of 5–10 ml 0.5 M $BaCl_2$ solution.

Sulfur and oxygen isotope ratios of samples were determined by continuous flow isotope ratio mass spectrometry (CF-IRMS) using an elemental analyzer ($\delta^{34}S_{H_2S}$, $\delta^{34}S_{SO_4}$) or a Thermo-Finnigan TC/EA at 1450 °C ($\delta^{18}O_{SO_4}$) coupled to a gas source mass spectrometer. Oxygen and sulfur isotope results are expressed relative to Vienna Standard Mean Ocean Water (V-SMOW) and Canyon Diablo Troilite (V-CDT), respectively, using the standard δ notation:

$$\delta^{34}S \text{ or } \delta^{18}O\ [‰] = [(R_{sample}/R_{standard}) - 1] \times 10^3 \quad (4)$$

where R are $^{34}S/^{32}S$ and $^{18}O/^{16}O$ of sample and standard, respectively. For sulfur isotope measurements, IAEA S1 (−0.3‰), S2 (+22.67‰), SO-5 (+0.49‰), and SO-6 (−34.05‰) were analyzed repeatedly for calibration and normalization purposes. Oxygen isotope ratios of sulfate were normalized to NBS 127 ($\delta^{18}O = +8.6$‰), SO-5 (+12.0‰), and SO-6 (−11.3‰). Reproducibility of the $\delta^{34}S$ and $\delta^{18}O$ values for sulfide and sulfate were generally better than ±0.5‰. Oxygen isotope ratios of water used in the experiments were determined repeatedly using standard equilibration techniques (Epstein and Mayeda, 1953) and found to be constant at −17.9 ± 0.3‰ with respect to Vienna Standard Mean Ocean Water (V-SMOW).

2.4. Sample selection for isotope analysis

In order to assess isotope effects in the bioreactors it was important to estimate the extent of BSR (the inverse of f) under different experimental conditions (i.e., at different NO_x doses). Apparent f values were calculated by comparing steady state sulfate concentrations at each sampling port with the sulfate concentration in batches of simultaneously inflowing medium. Sulfur balances for ports 2–5 and the bioreactor effluent yielded reliable apparent f values, however, this was not the case for port 1 where mixing of inflowing sulfate and produced sulfide made estimating apparent f problematic. Therefore, isotope analyses from the bioreactors were only considered for samples taken downstream from port 1. Although samples for isotope analyses were taken at every NO_x dose, some low doses (low apparent f) yielded insufficient barium sulfate for isotope analysis and some high doses (high apparent f) did not yield enough cadmium sulfide for isotope analysis.

3. RESULTS

Results of chemical and isotopic measurements associated with batch culture experiments, the nitrate-treated bioreactor and two nitrite-treated bioreactors are summarized in Tables 2–4, respectively.

Table 2
Chemical and isotope data from batch culture experiments.

Experiment	Time (h)	Sulfide (mM)	Sulfate (mM)	$\delta^{34}S_{H_2S}$ (‰)	$\delta^{34}S_{SO_4}$ (‰)	$\delta^{18}O_{SO_4}$ (‰)
Desulfovibrio (batch culture)						
	0.1	0.1	8.6	ND	+4.4	+10.3
	46.0	0.4	8.0	−3.5	+4.1	+9.1
	54.5	0.3	8.2	−3.6	+3.6	+9.6
	62.5	0.7	7.4	−4.1	+4.2	+9.0
	71.0	1.2	6.6	−4.4	+5.3	+9.1
	78.0	2.6	5.7	−4.4	+3.8	+8.8
	87.5	4.8	3.2	−3.9	+4.4	+8.4
	92.5	7.1	1.9	−2.4	+4.1	+8.0
	95.0	5.5	1.7	−1.1	+14.4	+8.4
	99.0	6.5	0.9	−0.3	+18.1	+9.6
	111.5	7.6	0.0	+3.2	ND	+11.5
Thiomicrospira (batch culture)						
	0.0	5.9	0.0	+0.9	ND	ND
	6.5	5.5	0.0	+0.2	ND	ND
	11.5	1.6	0.0	+0.5	ND	ND
	13.5	0.2	0.0	ND	ND	ND
	15.0	0.1	0.0	ND	ND	ND
	16.5	0.2	0.0	ND	ND	ND
	18.0	0.2	0.0	ND	ND	ND
	25.5	0.1	1.9	ND	−1.9	−17.3
	37.5	0.1	6.1	ND	+0.2	−18.1

Table 3
Chemical and isotope data from the nitrate-treated bioreactor.

NO_3^- dose (mM)	Sample location	Sulfide (mM)	Sulfate (mM)	$\delta^{34}S_{H_2S}$ (‰)	$\delta^{34}S_{SO_4}$ (‰)	$\delta^{18}O_{SO_4}$ (‰)
0	Medium	0.0	5.5	ND	+5.7	+9.5
0	Port 2	5.8	0.5	+6.9	ND	ND
0	Port 5	5.5	0.5	+6.9	ND	ND
2.5	Medium	0.0	5.8	ND	ND	+8.8
2.5	Port 2	5.6	1.8	+0.2	ND	ND
2.5	Port 3	5.7	1.8	+0.4	ND	ND
2.5	Port 4	5.7	1.9	+0.2	ND	ND
2.5	Port 5	5.7	1.9	+0.3	ND	ND
5	Medium	0.0	6.6	ND	+7.4	ND
5	Port 2	2.9	3.3	−9.0	+15.3	+7.8
5	Port 3	3.0	3.4	−8.8	+16.0	+7.0
5	Port 4	3.1	3.4	−8.4	+16.2	+7.0
5	Port 5	2.9	3.4	−7.4	+14.3	+7.7
7.5	Medium	0.0	6.1	ND	+6.3	+6.4
7.5	Port 2	0.6	5.6	−13.0	+7.5	+7.6
7.5	Port 3	0.6	5.6	−13.9	+8.7	+8.6
7.5	Port 4	0.6	5.6	−13.8	+7.8	+7.9
7.5	Port 5	0.6	5.5	−14.3	+7.8	ND
10	Medium	0.0	6.2	ND	+5.7	+7.8
10	Port 2	0.1	6.3	ND	+5.7	+8.1
10	Port 3	0.1	6.4	ND	+6.0	+7.9
10	Port 4	0.1	6.3	ND	+5.6	+8.3
10	Port 5	0.1	6.3	ND	+5.7	+8.6
12.5	Medium	0.0	5.7	ND	ND	+7.8
12.5	Port 2	0.1	6.2	ND	+6.1	+8.0
12.5	Port 3	0.2	6.1	ND	+5.7	+7.1
12.5	Port 4	0.1	6.1	ND	+5.9	+7.5
12.5	Port 5	0.1	6.1	ND	+6.2	ND
15	Medium	0.0	5.5	ND	+5.3	+7.0
15	Port 2	0.2	6.0	ND	+5.9	+8.0
15	Port 3	0.1	6.0	ND	+6.4	+7.8
15	Port 4	0.1	6.1	ND	+5.4	+8.0

3.1. Batch culture experiments

Pure cultures were selected for control experiments to determine sulfur and oxygen isotope effects associated with BSR and anaerobic sulfide oxidation with nitrate. *Desulfovibrio* sp. strain Lac15 was isolated from an oil field in Western Canada (Voordouw et al., 1992) and was shown to be an important member of the sulfate-reducing microbial community in bioreactors that received subsequent nitrate or nitrite treatments (Hubert et al., 2003, 2005; Hubert and Voordouw, 2007). *Thiomicrospira* sp. strain CVO was also isolated from an oil field in Western Canada where it was shown to be a dominant member of the microbial community following souring control by nitrate injection (Telang et al., 1997). When cultured in excess nitrate, strain CVO catalyses complete oxidation of sulfide to sulfate without intermediate S compounds accumulating in the medium (Greene et al., 2003). This makes CVO activity under these conditions (Table 1) appropriate for assessing our hypotheses by evaluating $\delta^{34}SO_{H_2S}$, $\delta^{34}S_{SO_4}$ and $\delta^{18}O_{SO_4}$ during NR-SOB metabolism.

Table 4
Chemical and isotope data from nitrite-treated bioreactors.

NO_2^- dose (mM)	Sample location[a]	Sulfide (mM)	Sulfate (mM)	$\delta^{34}S_{H_2S}$ (‰)	$\delta^{34}S_{SO_4}$ (‰)	$\delta^{18}O_{SO_4}$ (‰)
0	A; medium	0.0	8.2	ND	+5.8	+9.7
0	B; medium	0.0	8.3	ND	+5.8	+9.7
0	A; port 4	7.6	0.5	+7.8	+5.5	+5.1
0	B; port 4	7.8	0.6	+8.0	+6.0	+5.8
4	A; medium	0.0	8.6	ND	+6.5	+9.1
4	B; medium	0.0	8.7	ND	+6.2	+10.0
4	A; port 4	7.2	1.9	+3.1	+9.6	+7.3
4	B; port 4	7.3	1.0	+4.7	+5.8	+6.6
8	A; medium	0.0	8.4	ND	+5.8	+9.4
8	B; medium	0.0	8.3	ND	+6.5	+9.6
8	A; port 4	7.4	1.8	+5.6	+8.1	+6.4
8	B; port 4	5.9	2.3	+1.2	+9.8	+7.5
12	A; medium	0.0	7.7	ND	+6.3	+9.6
12	B; medium	0.0	8.2	ND	+6.0	+9.9
12	A; port 4	4.9	3.7	ND	+8.9	+7.9
12	B; port 4	5.3	3.5	−0.3	+9.1	+8.0
16	A; medium	0.0	7.7	ND	+5.9	+9.3
16	B; medium	0.0	8.4	ND	+6.3	+9.8
16	A; port 4	3.4	4.9	−3.0	+9.6	+8.6
16	B; port 4	3.1	4.8	−3.7	+9.0	+9.1
20[b]	A; medium	0.0	7.8	ND	+6.6	+9.7
20[b]	B; medium	0.0	8.0	ND	+6.3	+10.0
20[b]	A; port 4	1.4	6.1	−5.6	+9.0	+8.9
20[b]	B; port 4	0.2	7.3	−7.8	+7.7	+9.2
20[c]	B; medium	0.0	7.6	ND	+5.8	+12.6
20[c]	B; port 4	0.7	7.0	−10.0	+6.5	+12.1
20[d]	B; medium	0.0	8.2	ND	+5.8	+11.6
20[d]	B; port 4	0.6	7.4	−13.9	+7.2	+12.3

[a] Two bioreactors A and B received parallel nitrite treatments (Hubert et al., 2005).
[b] After 12 days of 20 mM nitrite addition, isotope samples were taken from both bioreactors and bioreactor A was stopped.
[c] Isotope analyses from bioreactor B after 45 days of 20 mM nitrite addition.
[d] Isotope analyses from bioreactor B after 71 days of 20 mM nitrite addition.

3.1.1. Isotope effects in SRB pure cultures

Desulfovibrio sp. strain Lac15 reduced sulfate completely to sulfide in medium with excess lactate as the electron donor (Table 1 and Fig. 3a). Isotope ratios revealed the expected Rayleigh fractionation of sulfur isotopes as f decreased from 1 to 0 with time, with initial sulfate in the culture medium having a $\delta^{34}S_{SO_4}$ value of +4‰ that increased to +20‰. Likewise, initially produced sulfide had a $\delta^{34}S_{H_2S}$ value of −4‰ that increased to +4‰ in the accumulated sulfide as the reaction progressed towards completion (Fig. 3b). The isotope data plotted in Fig. 3b correspond to a sulfur isotope enrichment factor (ϵ_s) of ca. −7‰ for strain Lac15 under these conditions. The $\delta^{18}O_{SO_4}$ values of the unreacted sulfate did not increase with respect to the initial $\delta^{18}O_{SO_4}$ value of +11‰, but remained constant at 9.0 ± 0.7‰ during BSR (Fig. 3c). Oxygen isotope effects associated with BSR were difficult to assess with the media used because the difference between starting $\delta^{18}O$

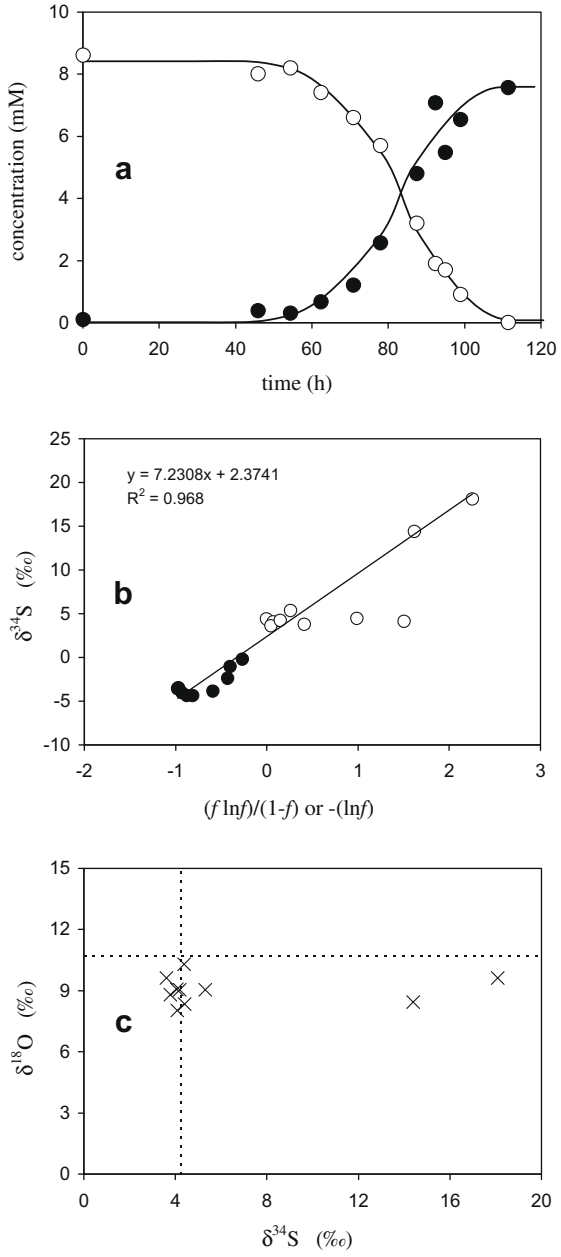

Fig. 3. Batch culture of *Desulfovibrio* sp. strain Lac15 in medium containing sulfate and lactate to promote SRB activity. (a) Concentrations of sulfide (●) and sulfate (○) monitored during a time series correspond with (b) $\delta^{34}S_{H_2S}$ values for produced sulfide (●) and $\delta^{34}S_{SO_4}$ values for unreacted sulfate (○), which are plotted as a function of $(f \ln f)/(1-f)$ and $(-\ln f)$, respectively, after Bolliger et al. (2001). The regression line indicates a sulfur isotope enrichment factor (slope) of 7.2‰ and was calculated by excluding two outlying $\delta^{34}S_{SO4}$ values (including these in the regression gives a slope of 6.1). Panel (c) plots $\delta^{18}O_{SO_4}$ against $\delta^{34}S_{SO_4}$ for all sulfate data (×) indicating that $\delta^{18}O_{SO_4}$ was constant (and coincidentally, close to the $\delta^{18}O_{mCSB-SO_4}$ value of +10.7‰; horizontal dashed line) while $\delta^{34}S_{SO_4}$ increased from initial $\delta^{34}S_{mCSB-SO_4}$ values (+4.3‰; vertical dashed line) during BSR. Isotope values are plotted for sulfate and sulfide for all time points where sulfate and sulfide concentrations (a) were greater than 0. All isotope values from this experiment are listed in Table 2.

values for sulfate (+11‰) and water (−18‰) was close to the value expected for equilibrium conditions (Fritz et al., 1989). Therefore, it is possible that equilibrium isotope exchange between intermediate sulfite and water followed by reverse reactions in the BSR pathway (Brunner et al, 2005; Mangalo et al., 2007) explain the lack of variation in $\delta^{18}O_{SO4}$.

3.1.2. Isotope effects in NR-SOB pure cultures

Monitoring sulfide oxidation to sulfate by *Thiomicrospira* sp. strain CVO showed that sulfide was initially oxidized to intermediate S compounds that were eventually oxidized further to sulfate (Fig. 4a). Possible intermediate compounds, such as polysulfides, elemental sulfur, thiosulfate and sulfite, were not quantitatively determined or extracted for isotope analyses. However a transient white–yellow suspension, presumably elemental sulfur, was observed in the experimental flasks between 10 and 20 h of incubation. $\delta^{34}S_{H_2S}$ values of unreacted sulfide remained close to the starting value of +1‰ (Fig. 4b) during conversion of sulfide to intermediate compounds (ca. 0–10 h; Fig. 4b), whereas produced sulfate initially had slightly

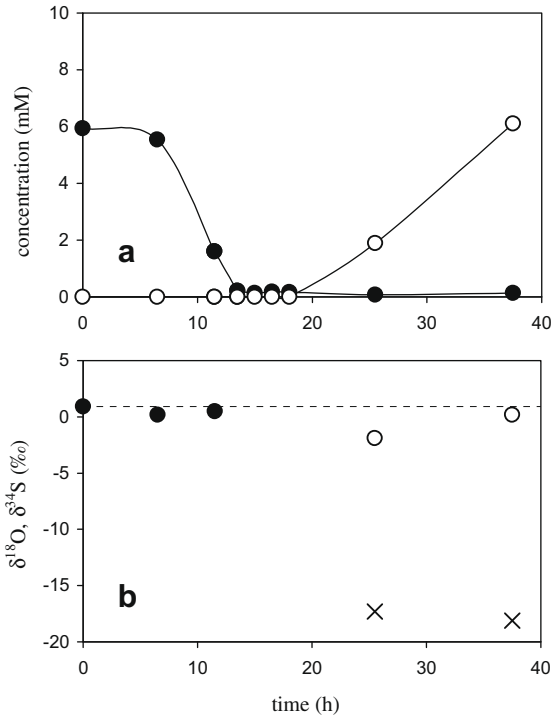

Fig. 4. Batch cultures of *Thiomicrospira* sp. strain CVO in medium containing sulfide and nitrate to promote NR-SOB activity. (a) Concentrations of sulfide (●) and sulfate (○) monitored during a time series correspond with (b) $\delta^{34}S_{H_2S}$ values for unreacted sulfide (●) as well as $\delta^{34}S_{SO_4}$ values (○) and $\delta^{18}O_{SO_4}$ values (×) determined for produced sulfate. The dashed line indicates the $\delta^{34}S_{H_2S}$ value of unreacted sulfide in CSB-A medium (+1‰) prior to inoculation of CVO cells. Isotope values are plotted when sulfate and sulfide concentrations (a) are greater than 0.2 mM. All isotope values from this experiment are listed in Table 2. Nitrate was reduced in stoichiometric amounts, as described elsewhere (Greene et al., 2003; data not shown).

lower $\delta^{34}S_{SO_4}$ (−2‰) and approached +1‰ as the reaction progressed towards completion (Fig. 4b). This limited data set suggests that no significant S isotope fractionation occurs during the initial step of sulfide oxidation to intermediate S compounds by strain CVO. However, the subsequent conversion of S intermediates into sulfate appears to be associated with a small S isotope fractionation.

The sulfate produced by strain CVO had a $\delta^{18}O_{SO_4}$ value near −18‰, which matches the $\delta^{18}O_{H_2O}$ value of the CSB-A medium used (−17.9 ± 0.3‰). This indicates that during anaerobic sulfide oxidation to sulfate by NR-SOB the four new oxygen atoms incorporated into the sulfate molecule are derived from water. This is similar to results of pyrite (FeS_2) oxidation experiments under similar conditions (Balci et al., 2007 and references therein). Oxygen isotope exchange between water and sulfate produced by strain CVO does not occur under these experimental conditions within the time-scale shown in Fig. 4 (Chiba and Sakai, 1985). Therefore, sulfate generated via sulfide oxidation in our CSB medium experiments is characterized by a markedly lower $\delta^{18}O_{SO_4}$ value (ca. −18‰; Fig. 4b) than sulfate that has only been influenced by BSR (⩾+8‰; Fig. 3c).

3.2. Bioreactor experiments

Steady state chemical profiles from the souring control bioreactor experiments after each nitrate and nitrite amendment are summarized in Fig. 5. More detailed profiles and descriptions of these results, as well as corresponding molecular microbial community analyses, can be found elsewhere for the nitrate-treated bioreactor (Hubert and Voordouw, 2007) and the nitrite-treated bioreactors (Hubert et al., 2005).

3.2.1. Control of sulfide production in experimental bioreactors

Prior to introducing nitrate or nitrite into the bioreactors, SRB coupled the incomplete oxidation of lactate to acetate and CO_2, with the reduction of sulfate to sulfide, as follows:

$$2C_3H_6O_3 + SO_4^{2-} + 2H^+ \rightarrow 2C_2H_4O_2 + 2CO_2 + H_2S + 2H_2O \quad (5)$$

This stoichiometry shows that these SRB oxidize two lactate per sulfate reduced. Therefore, bioreactor mCSB medium always contained >2-fold more lactate than sulfate to ensure that all sulfate was reduced ($f = 0$) prior to nitrate or nitrite (NO_x) being introduced (Fig. 5 and Table 1). Lactate was in greater excess in the mCSB media introduced to the nitrite-treated bioreactors (Table 1), hence similar NO_x amounts resulted in different degrees of sulfide elimination (different apparent f; Fig. 5c). Increasing amounts of NO_x initially stimulated oxidation of the excess lactate, and eventually resulted in net oxidation of lactate by NO_x instead of by sulfate reduction (Hubert et al., 2005; Hubert and Voordouw, 2007). This shift is indicated by the change in sulfate and sulfide concentrations (i.e., increases in apparent f) during addition of 5–7.5 mM nitrate (Fig. 5a) and of 4–20 mM nitrite (Fig. 5b). Under these conditions sulfate appears to no longer be completely reduced to sulfide (apparent $f > 0$), whereas the added dose of nitrate or nitrite was always completely consumed (data not shown; see Hubert et al. 2005 and Hubert and Voordouw, 2007). In the presence of sulfate and introduced NO_x, lactate was always completely consumed yielding stoichiometric amounts of acetate (data not shown; see Hubert et al., 2005; Hubert and Voordouw, 2007), further indicating that

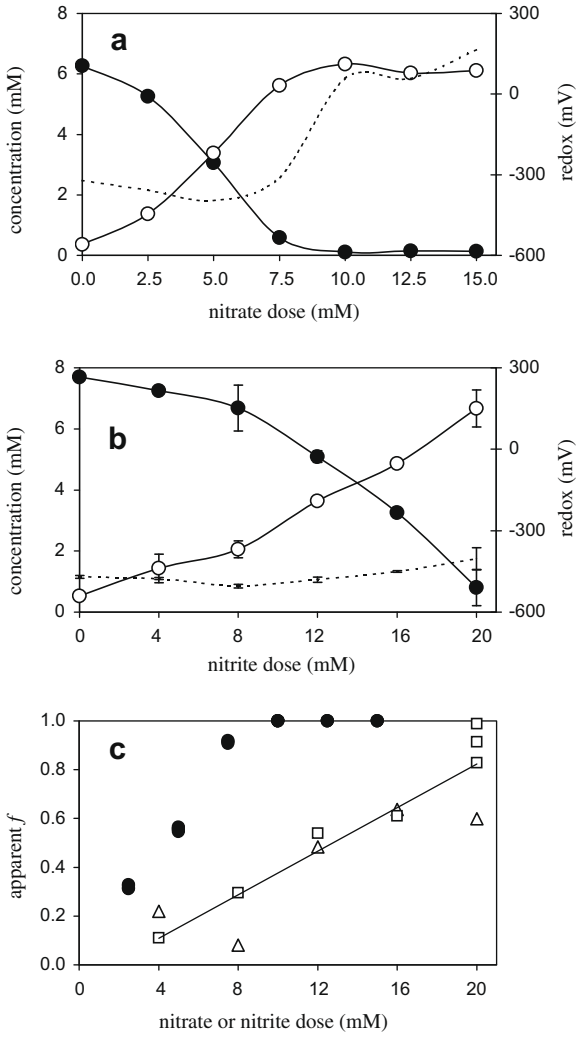

Fig. 5. Chemical concentration profiles obtained at sampling port 4 from different bioreactors that plot steady state sulfate (○) and sulfide (●) concentrations as well as redox potential (- - - -) as a function of (a) nitrate and (b) nitrite dose. For the nitrite treatment, average values for the two bioreactors are plotted (b) with vertical bars representing the standard error. Port 4 was chosen to represent ports 2–5 which were always similar. More detailed chemical profiles have been reported previously for the nitrate-treated bioreactor ((a); Hubert and Voordouw, 2007) and the two nitrite-treated bioreactors ((b); Hubert et al., 2005). The disappearance of sulfide (apparent $f = 1$) was facilitated by different doses of nitrate (7.5 mM) and nitrite (20 mM) due to the use of 12.5 and 25 mM lactate used in respective mCSB media (Table 1; Hubert et al., 2003; see Section 4.4). This difference is illustrated in (c) where apparent f conditions promoted by the nitrate (●) and nitrite (bioreactor A = △; bioreactor B = □) dosing regimes are plotted.

the SRB and/or O-NRB were incomplete oxidizers and that acetate-oxidizers were not active in the bioreactor microbial communities.

3.2.2. Isotope effects in the nitrate-treated bioreactor

The mean $\delta^{34}S_{SO_4}$ value of mCSB supplied to the nitrate-treated bioreactor was $+6.1 \pm 0.8‰$ ($n = 5$ different batches of mCSB; Table 1) as indicated by the dashed lines in Fig. 6a. Prior to nitrate addition $\delta^{34}S_{H_2S}$ values of produced sulfide also fell within the same range indicating complete conversion of the initial sulfate by BSR ($f = 0$). As the nitrate dose increased (i.e., as apparent f increased from 0 towards 1) $\delta^{34}S_{H_2S}$ values became more negative displaying Rayleigh-type trends characteristic for incomplete BSR

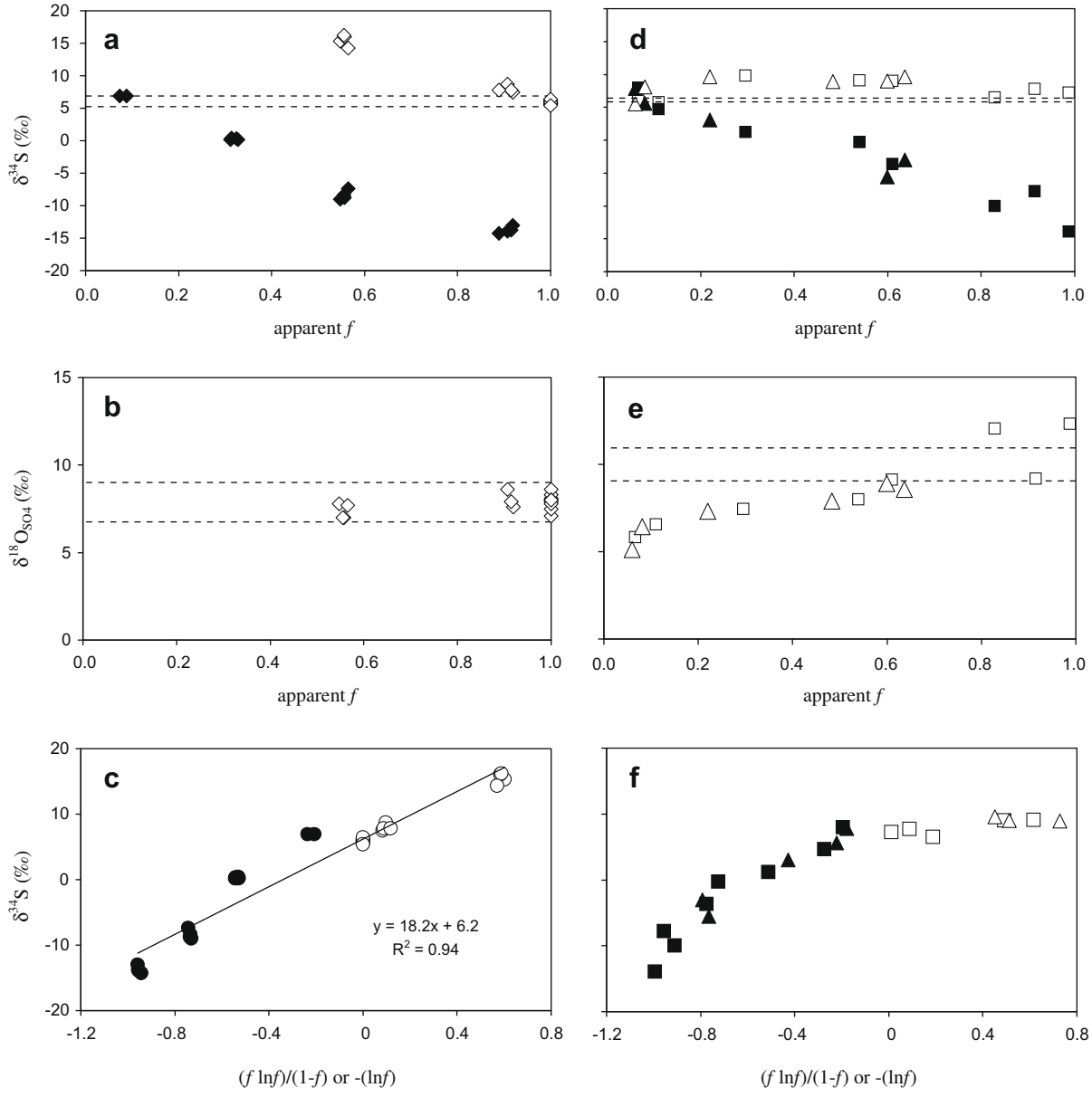

Fig. 6. Isotope values for sulfate (open symbols) and sulfide (filled symbols) measured in the bioreactors treated with nitrate (a–c) or nitrite (d–f). Values of $\delta^{34}S_{H_2S}$ and $\delta^{34}S_{SO_4}$ (a and d) and $\delta^{18}O_{SO_4}$ (b and e) are plotted against the apparent f, which increases in response to step-wise NO_x addition (cf. Fig. 5c). Results from the nitrate-treated bioreactor correspond to samples obtained at ports 2–5. Results from the two nitrite-treated bioreactors correspond to samples only from port 4 and are plotted using separate symbols (bioreactor A = △; bioreactor B = □). Horizontal dashed lines (a, b, d, e) represent standard deviations around mean values for $\delta^{34}S_{SO_4}$ and $\delta^{18}O_{SO_4}$ in mCSB media based on $n = 5$ (a), $n = 6$ (b) and $n = 14$ (d and e) replicate medium batches. Panels (c) and (f) show $\delta^{34}S_{SO_4}$ data plotted as a function of $(-\ln f)$ and $\delta^{34}S_{H_2S}$ data as a function of $(f \ln f)/(1 - f)$, after Bolliger et al. (2001). A regression line is shown for the nitrate-treated bioreactor data (c), indicating a Rayleigh-type isotope pattern with an isotope enrichment factor (slope) of 18.2‰. The non-linear profile obtained from the bioreactors treated with nitrite (f) suggests non-Rayleigh-type isotope effects. Isotope values from bioreactors treated with nitrate and nitrite are listed in Tables 3 and 4, respectively.

(Fig. 6a). This corresponded with $\delta^{34}S_{SO_4}$ values as high as +15‰ measured during addition of 5 mM nitrate. Once high nitrate doses ($\geqslant$7.5 mM) achieved a decrease in sulfide to near zero and restored initial sulfate levels (Fig. 5a), $\delta^{34}S_{SO_4}$ decreased to +6‰ (Fig. 6a). The Rayleigh-type behaviour of S isotopes in the nitrate-treated bioreactor is further evident in Fig. 6c, which shows a near perfect linear fit of the data. Isotope ratios plotted in this way (Bolliger et al., 2001) allow comparative assessment of different batch and bioreactor experiments (Figs. 3c and 6c and f) with respect to Rayleigh isotope fractionation hypotheses (=biocompetitive exclusion, according to Fig. 1a; see Section 1.3). In instances where the Rayleigh hypothesis is supported by a linear fit of the data, an isotope enrichment factor can be calculated from the slope of the linear regression (Bolliger et al., 2001), which was −18.2‰ in the nitrate-treated bioreactor (Fig. 6c).

While $\delta^{34}S_{H_2S}$ and $\delta^{34}S_{SO_4}$ values varied in response to the nitrate treatment $\delta^{18}O_{SO_4}$ values remained constant at +7.8 ± 0.5‰ (Fig. 6b), which was similar to the oxygen isotope ratios of sulfate in the inflowing medium (+7.9 ± 1.1‰; $n = 6$ mCSB batches; Table 1).

3.2.3. Isotope effects in nitrite-treated bioreactors

Isotope data from the nitrite-treated bioreactors are plotted in Fig. 6d–f. As the nitrite dose (hence apparent f) increased $\delta^{34}S_{H_2S}$ values became more negative (Fig. 6d). While this trend is similar to that observed during nitrate addition, there are notable differences in the isotope profiles between nitrate and nitrite treatments. During introduction of low nitrite concentrations (smaller apparent f) $\delta^{34}S_{H_2S}$ values of sulfide were close to those of the initial sulfate (+6‰), but $\delta^{34}S_{SO_4}$ values of the remaining sulfate did not show strong ^{34}S enrichment typical of BSR approaching completion in closed systems (e.g., Fig. 3b). Instead, $\delta^{34}S_{SO_4}$ values associated with low apparent f were also close to those of the initial sulfate. The S isotope pattern promoted by the nitrite treatments (Fig. 6d) does not resemble a Rayleigh-type scenario as seen with nitrate (Fig. 6a). This is also demonstrated by the non-linear plot in Fig. 6f. The convergence of $\delta^{34}S_{SO_4}$ and $\delta^{34}S_{H_2S}$ values at lower nitrite doses (=low apparent f) observed in Fig. 6d is also illustrated in Fig. 7, which plots the difference between $\delta^{34}S_{SO_4}$ and $\delta^{34}S_{H_2S}$ ($\Delta^{34}S_{SO_4-H_2S}$) in relation to apparent f. In the nitrate-treated bioreactor $\Delta^{34}S_{SO_4-H_2S}$ could only be calculated for experimental conditions of apparent $f \geqslant 0.5$, and was relatively constant between 20‰ and 25‰. During nitrite addition, $\Delta^{34}S_{SO_4-H_2S}$ exhibited a positive correlation with apparent f (hence with the nitrite dose), increasing from 1‰ at low apparent f to a maximum of 22‰ at high apparent f (20 mM nitrite).

Unlike the nitrate-treated bioreactor that exhibited constant $\delta^{18}O_{SO_4}$ values, a decreasing trend was observed in the $\delta^{18}O_{SO_4}$ values in the nitrite-treated bioreactors with decreasing apparent f. During dosing with low nitrite concentrations that promoted conditions of low apparent f, $\delta^{18}O_{SO_4}$ values were near +5‰ (Fig. 6e). As the nitrite dose increased and the apparent f became >0.6, the $\delta^{18}O_{SO_4}$ values increased to levels similar to those of the initial mCSB sulfate of +10.0 ± 0.9‰ ($n = 14$ mCSB batches; Table 1).

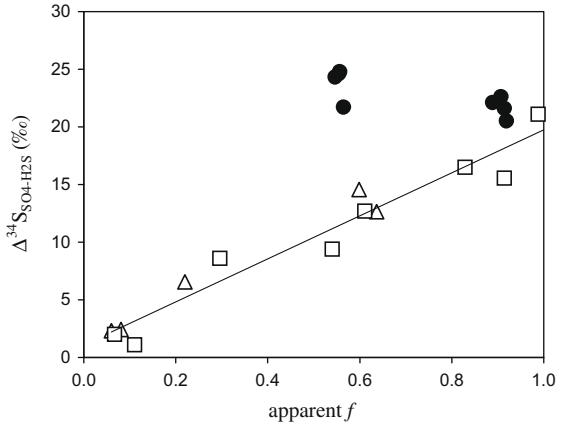

Fig. 7. Differences between $\delta^{34}S_{SO_4}$ and $\delta^{34}S_{H_2S}$ in the same sample ($\Delta^{34}S_{SO_4-H_2S}$), are plotted against the apparent f for the bioreactor treated with nitrate (●) and the two bioreactors treated with nitrite (bioreactor A = △; bioreactor B = □). The regression line was calculated using all $\Delta^{34}S_{H_2S-SO_4}$ values from both nitrite-treated bioreactors.

4. DISCUSSION

4.1. Comparison of batch and bioreactor experimental systems

In order to interpret the isotope results from the flow-through bioreactors in light of the isotope results from the batch culture controls, it is important to consider whether and how these systems can be compared. Steady state conditions were established at all sampling ports in the bioreactors at each NO_x dose prior to sampling for chemical and isotope analyses. This ensured that the sulfate and sulfide concentrations as a function of the NO_x doses in the bioreactors were comparable to sulfate and sulfide concentrations as a function of time in closed batch culture systems. This is illustrated by comparing Fig. 3a and Fig. 5 which show similar sulfate and sulfide dynamics as a function of time and NO_x dose, respectively; the *Desulfovibrio* pure culture profile as a function of time is the reverse of bioreactor chemical profiles as a function of NO_x dose (Figs. 3a, and 5a and b). Increasing NO_x doses promote conditions where sulfide concentrations are low, which are comparable to conditions in a sulfate-reducing batch culture during the initial hours when BSR is just beginning. The trends shown in Figs. 3a and 5 are the same if time and NO_x on the x-axis are substituted with f or apparent f, respectively. From Fig. 5 it can be seen that the NO_x dose directly alters the S balance. Since f is generally defined as C_t/C_0, the NO_x dose determines f, or apparent f. The amount of sulfide in the system thus depends on the amount of NO_x added. However, whether or not shifts in f are real or only 'apparent' depends on whether the active NRB are organotrophic or lithotrophic (Fig. 1). The physiology of the active NRB determines how nitrate or nitrite reduction achieves the observed changes in chemical

parameters (Fig. 5). Stable isotope ratios reveal the predominant process as explained below.

4.2. Isotope effects during biocompetitive exclusion of SRB by organotrophic NRB

4.2.1. Predicted isotope effects during biocompetitive exclusion

The chemical patterns summarized in Fig. 5 can be explained by the biocompetitive exclusion of SRB by lactate-oxidizing O-NRB. This would proceed in two phases. Phase 1: O-NRB activity consumes part of the lactate that was originally present in excess, given a lactate-to-sulfate ratio >2 (required for complete BSR; Eq. (5)). NO_x reduction does not affect S and O isotope ratios in sulfate and sulfide, but it decreases the lactate-to-sulfate ratio to <2. Phase 2: BSR proceeds via the oxidation of lactate left over from phase 1. The excess reactant is now sulfate, not lactate, which promotes partial BSR ($f > 0$). This results in kinetic sulfur isotope fractionation affecting both the newly formed sulfide and the remaining sulfate (Fig. 3b). As the NO_x dose increases, the lactate-to-sulfate ratio decreases further (during phase 1), thereby reducing the extent of BSR (during phase 2). In this Rayleigh-type scenario, the apparent f parameter is also the actual f that governs the observed S isotope fractionation. The S isotope ratios are thus different for each NO_x dose. Oxygen isotope ratios in unreacted sulfate are expected to show no change, in agreement with the $\delta^{18}O$ values of initial sulfate (+6‰) and water (−18‰) being close to equilibrium (Fritz et al., 1989) as observed in the BSR control culture (Fig. 3c).

Predicted reactions and isotope effects for phases 1 and 2 are shown in Table 5 for a scenario where souring control is due exclusively to O-NRB catalyzing biocompetitive exclusion in response to a representative NO_x dosing regime. Predicted isotope trends are further depicted in Fig. 8, which shows a reverse Rayleigh-type profile as a function of NO_x dose (dashed lines; Fig. 8).

4.2.2. Interpretation of isotope effects in the nitrate-treated bioreactor

Collectively, $\delta^{34}S$ and $\delta^{18}O$ values for the nitrate-treated bioreactor are in good agreement with the isotope effects observed in the BSR control culture (Fig. 3) and the predicted trends for the biocompetitive exclusion mechanism (Section 4.2.1; Fig. 8). Fig. 6a shows the predicted reverse Rayleigh-type S isotope pattern, and comparing Fig. 6c with Fig. 3b reveals similar S isotope effects. Moreover $\delta^{18}O_{SO_4}$ values of the remaining sulfate were constant in both cases (Figs. 3c and 6b). This demonstrates that SRB were out-competed by O-NRB as depicted in Fig. 1a, preventing BSR and resulting in the disappearance of sulfide.

4.2.3. Sulfur isotope fractionation during bacterial sulfate reduction

The sulfur isotope fractionation associated with BSR during intermediate nitrate dosing in the bioreactor (Fig. 6a) was much greater than that observed in the batch culture of *Desulfovibrio* strain Lac15 (Fig. 3b and c). The data plotted in Fig. 6c correspond to an ϵ_s for the bioreactor SRB community of −18.2‰ under these experimental conditions. Detmers et al. (2001) reported ϵ_s between −2.0‰ and –17.0‰ for 14 sulfate-reducing pure cultures catalyzing incomplete oxidation of lactate to acetate and CO_2. Our result for strain Lac15 (an incomplete oxidizer) falls near the lower end of this range (−7‰; Fig. 3b), whereas the −18.2‰ for the SRB community in the nitrate-treated bioreactor (Fig. 6c) exceeds this range. Reverse sample genome probing indicated that strain Lac15 was a dominant sulfate reducer in the nitrate-injected bioreactor microbial community (Hubert and Voordouw, 2007). However, other SRB may also have been enriched from the produced water inoculum and contributed to the observed BSR as well. Activity of a mixed SRB population may have promoted greater sulfur isotope fractionation. Other possible explanations for the larger ϵ_s could be related to the bioreactor experiment representing natural conditions more accurately than the batch culture experiment. Bioreactor SRB were presumably present in biofilms, which may promote activities that influence ϵ_s differently than those of planktonic SRB in often-studied liquid cultures. Another interesting possibility relates to the microbial ecology of biocompetitive exclusion and whether competing for organic electron donors with other microbes (e.g., O-NRB) promotes larger sulfur isotope fractionations during sulfate respiration.

4.3. Isotope effects during oxidation of sulfide by lithotrophic NR-SOB

4.3.1. Predicted isotope effects during anaerobic sulfide oxidation

Chemical profiles indicative of souring control (e.g., Fig. 5) can also be explained by NR-SOB that reoxidize sulfide produced by SRB back to sulfate. In the presence of excess NO_x, this can create a continuous sulfur cycle (Fig. 1b) whereby SRB and NR-SOB are mutually co-existent. In such a scenario, the NO_x-dependent increase in apparent f is somewhat misleading, since complete reduction of the original sulfate in the medium is always being maintained (actual $f = 0$). Resulting sulfide and sulfate pools would thus be characterized by isotopic compositions determined by the NR-SOB and SRB reactions outlined in Table 5, which can be conceptualized in different phases. Phase 1: complete BSR occurs in the presence of excess lactate such that the sulfur isotope ratio of the produced H_2S is identical to that of the initial sulfate. Phase 2: oxidation of sulfide back to sulfate by NR-SOB is associated with a small or negligible S isotope effect (Fig. 4b); the amount of sulfide oxidized and sulfate produced during phase 2 depends on the oxidative equivalent in the NO_x dose. Phase 3: un-oxidized lactate left over after phase 1 and sulfate produced by NR-SOB during phase 2 allow further BSR. The amount of lactate left over from phase 1 is determined by the sulfate concentration in the initial medium (constant, regardless of the NO_x; Table 1), however, the amount of sulfate regenerated in phase 2 and available for BSR in phase 3 depends directly on the NO_x dose. Hence at different NO_x doses, phase 3 BSR proceeds from different initial lactate-to-sulfate ratios (which decrease with increasing NO_x). Sulfur isotope fractionation during phase 3 will only influence

Table 5
Predicted reaction chemistries and isotope effects during sulfide removal via nitrite reduction[a] to reduced nitrogen species (N_{red}).

$[NO_2^-]$ (mM)	NRB[b]	Reaction chemistry[c]	^{18}O effect	% S pool[d]	f[e]	^{34}S effect	$\Delta^{34}S_{SO_4-H_2S}$ (‰)[f]
0		Overall: $0NO_2^- + 8SO_4^{2-} + 25Lac \rightarrow 0N_{red} + 8S^{2-} + 16(Ace + CO_2) + 9Lac$	None	100	0.00	None	0
4		Overall: $4NO_2^- + 8SO_4^{2-} + 25Lac \rightarrow 4N_{red} + 8S^{2-} + 20.8(Ace + CO_2) + 4.2Lac$					
	O-NRB	Phase 1: $4NO_2^- + 25Lac \rightarrow 4N_{red} + 4.8(Ace + CO_2) + 20.2Lac$	—	—	—	—	0
		Phase 2: $8SO_4^{2-} + 20.2Lac \rightarrow 8S^{2-} + 16(Ace + CO_2) + 4.2Lac$	None	100	0.00	None	
	NR-SOB	Phase 1: $8SO_4^{2-} + 25Lac \rightarrow 8S^{2-} + 16(Ace + CO_2) + 9Lac$	None	100	0.00	None	0
		Phase 2: $4NO_2^- + 8S^{2-} \rightarrow 2.4SO_4^{2-} + 5.6\ S^{2-} + 4N_{red}$	[g]H_2O into SO_4	100	—	Negligible	
		Phase 3: $2.4SO_4^{2-} + 9Lac \rightarrow 2.4S^{2-} + 4.8(Ace + CO_2) + 4.2Lac$	None	30	0.00	None	
8		Overall: $8NO_2^- + 8SO_4^{2-} + 25Lac \rightarrow 8N_{red} + 7.7S^{2-} + 0.3SO_4^{2-} + 25(Ace + CO_2)$					
	O-NRB	Phase 1: $8NO_2^- + 25Lac \rightarrow 8N_{red} + 9.6(Ace + CO_2) + 15.4Lac$	—	—	—	—	68.2
		Phase 2: $8SO_4^{2-} + 15.4Lac \rightarrow 7.7S^{2-} + 0.3SO_4^{2-} + 15.4(Ace + CO_2)$	Equilibrium	100	0.04	Kinetic	
	NR-SOB	Phase 1: $8SO_4^{2-} + 25Lac \rightarrow 8S^{2-} + 16(Ace + CO_2) + 9Lac$	None	100	0.00	None	57.7
		Phase 2: $8NO_2^- + 8S^{2-} \rightarrow 4.8SO_4^{2-} + 3.2S^{2-} + 8N_{red}$	H_2O into SO_4	100	—	Negligible	
		Phase 3: $4.8SO_4^{2-} + 9Lac \rightarrow 4.5S^{2-} + 0.3SO_4^{2-} + 9(Ace + CO_2)$	Equilibrium	60	0.06	Kinetic	
12		Overall: $12NO_2^- + 8SO_4^{2-} + 25Lac \rightarrow 12N_{red} + 5.3S^{2-} + 2.7SO_4^{2-} + 25(Ace + CO_2)$					
	O-NRB	Phase 1: $12NO_2^- + 25Lac \rightarrow 12N_{red} + 14.4(Ace + CO_2) + 10.6Lac$	—	—	—	—	32.8
		Phase 2: $8SO_4^{2-} + 10.6Lac \rightarrow 5.3S^{2-} + 2.7SO_4^{2-} + 10.6(Ace + CO_2)$	Equilibrium	100	0.34	Kinetic	
	NR-SOB	Phase 1: $8SO_4^{2-} + 25Lac \rightarrow 8S^{2-} + 16(Ace + CO_2) + 9Lac$	None	100	0.00	None	29.6
		Phase 2: $12NO_2^- + 8S^{2-} \rightarrow 7.2SO_4^{2-} + 0.8S^{2-} + 12N_{red}$	H_2O into SO_4	100	—	Negligible	
		Phase 3: $7.2SO_4^{2-} + 9Lac \rightarrow 4.5S^{2-} + 2.7SO_4^{2-} + 9(Ace + CO_2)$	Equilibrium	90	0.38	Kinetic	
16		Overall: $16NO_2^- + 8SO_4^{2-} + 25Lac \rightarrow 16N_{red} + 2.9S^{2-} + 5.1SO_4^{2-} + 25(Ace + CO_2)$					
	O-NRB	Phase 1: $16NO_2^- + 25Lac \rightarrow 16N_{red} + 19.2(Ace + CO_2) + 5.8Lac$	—	—	—	—	24.8
		Phase 2: $8SO_4^{2-} + 5.8Lac \rightarrow 2.9S^{2-} + 5.1SO_4^{2-}$	Equilibrium	100	0.64	Kinetic	
	NR-SOB	Phase 1: $8SO_4^{2-} + 25Lac \rightarrow 8S^{2-} + 16(Ace + CO_2) + 9Lac$	None	100	0.00	None	20.2
		Phase 2: $16NO_2^- + 8S^{2-} \rightarrow 8SO_4^{2-} + 13.3N_{red} + 2.7NO_2^-$	H_2O into SO_4	100	—	Negligible	
		Phase 3: $8SO_4^{2-} + 9Lac \rightarrow 4.5S^{2-} + 3.5SO_4^{2-} + 9(Ace + CO_2)$	Equilibrium	100	0.44	Kinetic	
		Phase 4: $2.7NO_2^- + 4.5S^{2-} \rightarrow 1.6SO_4^{2-} + 2.9S^{2-} + 2.7N_{red}$	H_2O into SO_4	56	—	Negligible[h]	
20		Overall: $20NO_2^- + 8SO_4^{2-} + 25Lac \rightarrow 20N_{red} + 0.5S^{2-} + 7.5SO_4^{2-} + 25(Ace + CO_2)$					
	O-NRB	Phase 1: $20NO_2^- + 25Lac \rightarrow 20N_{red} + 24(Ace + CO_2) + 1Lac$	—	—	—	—	20.7
		Phase 2: $8SO_4^{2-} + 1Lac \rightarrow 0.5S^{2-} + 7.5SO_4^{2-} + 1(Ace + CO_2)$	Equilibrium	100	0.94	Kinetic	
	NR-SOB	Phase 1: $8SO_4^{2-} + 25Lac \rightarrow 8S^{2-} + 16(Ace + CO_2) + 9Lac$	None	100	0.00	None	13.7
		Phase 2: $20NO_2^- + 8S^{2-} \rightarrow 8SO_4^{2-} + 13.3N_{red} + 6.7NO_2^-$	H_2O into SO_4	100	—	Negligible	
		Phase 3: $8SO_4^{2-} + 9Lac \rightarrow 4.5S^{2-} + 3.5SO_4^{2-} + 9(Ace + CO_2)$	Equilibrium	100	0.44	Kinetic	
		Phase 4: $6.7NO_2^- + 4.5S^{2-} \rightarrow 4.0SO_4^{2-} + 0.5S^{2-} + 6.7N_{red}$	H_2O into SO_4	56	—	Negligible[h]	

[a] Similar trends can be predicted for nitrate reduction, using a slightly different stoichiometry (1.4 lactate oxidized per nitrate reduced, instead of 1.2 lactate per nitrite Hubert et al., 2003).
[b] NRB physiology is either entirely organotrophic (O-NRB) or lithotrophic (NR-SOB) in the scenarios shown.
[c] Assuming 1.2 lactate oxidized per nitrite reduced (Fig. 5b; Hubert et al., 2003, 2005) and 0.6 sulfide oxidized per nitrite reduced. Lac, lactate; Ace, acetate; N_{red}, products of nitrite reduction.
[d] Proportion of the total sulfur pool (8 mM) being acted upon by the reaction chemistry indicated.
[e] The extent of BSR as determined by the specific reaction chemistry indicated.
[f] Predicted difference in bulk sulfate and sulfide isotope values between overall O-NRB and NR-SOB scenarios at each nitrite dose, assuming ϵ_s is 20‰.
[g] Sulfate produced during sulfide oxidation by NR-SOB will have an oxygen isotope value that is similar to the isotopic composition of the water in the medium (−18‰).
[h] The sulfide produced by partial BSR (phase 3) undergoes a negligible isotope effect during oxidation to sulfate (phase 4). Therefore, the new sulfate will assume low ^{34}S values consistent with those of the (^{32}S-enriched) parent sulfide.

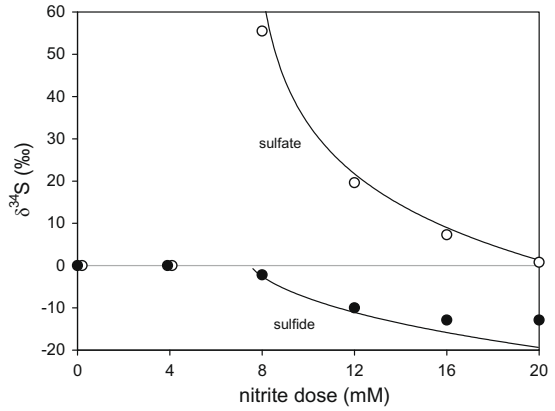

Fig. 8. Predicted S isotope effects for addition of different nitrite concentrations to a sulfidogenic bioreactor fed with mCSB medium containing 8 mM sulfate and 25 mM lactate. Anticipated isotope effects for sulfide elimination due exclusively to O-NRB that outcompete SRB for lactate are depicted by curved lines that resemble a reverse Rayleigh-type profile. These were obtained by calculating expected *f* for each nitrite dose by assuming 1.2 lactate are oxidized (to acetate and CO_2) per nitrite reduced (Table 5; Hubert et al., 2003), and applying a S isotope enrichment factor of 20‰ (similar to the nitrate-treated bioreactor; Fig. 6c; Section 4.2.3). The curved lines are best fits to data points for each nitrite dose (not shown). The same stoichiometry was assumed to predict isotope effects for sulfide elimination due exclusively to lithotrophic NR-SOB (Table 5), which are plotted for each nitrite concentration (circles). Predicted values of $\delta^{34}S$ for sulfate (○) and sulfide (●) correspond to the overall effect of sulfide oxidation and BSR that proceed to varying extents, as outlined in Table 5 and described in Section 4.3.1. All isotope values and trends are plotted relative to the initial $\delta^{34}S_{SO_4}$ for the mCSB medium, which is set to zero in this model (horizontal line).

a fraction of the sulfide and sulfate pools, with their relative sizes and the *f* governing BSR being determined by the NO_x dose. Accordingly, changes in $\delta^{34}S$ values associated with sulfide oxidation by NR-SOB are predicted to be smaller, at given NO_x doses, than those promoted by biocompetitive exclusion. Phase 4: at high NO_x doses (resulting in sulfide elimination; Fig. 5) leftover NO_x from phase 2 and sulfide produced during phase 3 enable further NR-SOB activity resulting in net complete sulfide removal.

Oxygen isotope effects associated with NR-SOB activity are expected to result in different $\delta^{18}O_{SO_4}$ values for sulfate compared to those observed during biocompetitive exclusion. As demonstrated for *Thiomicrospira* sp. strain CVO (Fig. 4b), incorporation of water oxygen results in very negative $\delta^{18}O_{SO_4}$ values for newly formed sulfate (phases 2 and 4); in our experiments this value was ca. −18‰. This is markedly different from $\delta^{18}O_{SO_4}$ values of the initial bioreactor sulfate (ca. +8‰ to +10‰; Table 1 and Fig. 6). BSR occurring during phases 1 and 3 is not expected to significantly affect $\delta^{18}O_{SO_4}$ values of the remaining sulfate as previously explained (Section 3.1.1; Fig. 3c; Table 5).

Reactions corresponding to phases 1–4 for NR-SOB were considered for the scenario of the nitrite-treated bioreactors (25 mM lactate and 8 mM sulfate; 4 mM nitrite increments; Table 1) and assuming an overall net reaction (Fig. 1b) of 1.2 mol lactate oxidized (to acetate and CO_2, a 4 electron transfer) per mol nitrite reduced (Fig. 5b; Hubert et al., 2003, 2005; Table 5). For NR-SOB activity, this corresponds with a direct oxidation of 0.60 mol sulfide to sulfate (8 electron transfer) per mol nitrite reduced. Predicted chemical and isotope results assuming souring control due exclusively to lithotrophic NR-SOB are summarized in Table 5. Profiles of the predicted isotope ratios as a function of nitrite dose are shown in Fig. 8. Table 5 and Fig. 8 thus allow comparison of isotope effects predicted for souring control due to either biocompetitive exclusion or NR-SOB activity.

4.3.2. Interpretation of isotope effects in the nitrite-treated bioreactor

Sulfur isotope fractionation was significantly higher at high nitrite doses compared to low nitrite doses (Fig. 6d). At high nitrite doses (high apparent *f*), the observed sulfur isotope effects were similar to the results of the nitrate treatment, with $\Delta^{34}S_{SO_4-H_2S}$ approaching the 20–25‰ range observed in the nitrate-treated bioreactor (Fig. 7). Nitrite has been shown to increase sulfur isotope fractionations in pure cultures of SRB (Mangalo et al., 2008) due to its ability to inhibit the dissimilatory sulfite reductase enzyme (DsrAB; Haveman et al., 2004; Greene et al., 2006). However, the nitrite introduced to these bioreactors was always consumed by nitrite-reducing bacteria, even when added in high doses (Hubert et al., 2005). Thus nitrite exerted influence on $\Delta^{34}S_{SO_4-H_2S}$ by stimulating NRB (Fig. 1), rather than as an inhibitor of BSR. $\delta^{18}O_{SO_4}$ values in the nitrite-treated bioreactors were close to those of initial sulfate at high nitrite doses (Fig. 6e). These observations suggest that biocompetitive exclusion occurred at high nitrite doses.

Isotope effects observed during addition of low nitrite concentrations were different. The difference between $\delta^{34}S$ values of sulfide and sulfate was smaller (Figs. 6d and 7), whereas $\delta^{18}O_{SO_4}$ decreased to values several per mill lower than that of original medium sulfate. These observations agree with predicted isotope effects if some NR-SOB activity and hence nitrite- and lactate-driven sulfur cycling (Fig. 1b) was occurring in the bioreactors. The oxygen isotope results indicate that the relative contribution of NR-SOB to the removal of sulfide from these systems appears to decline as the nitrite dose increases. The lowest measured $\delta^{18}O_{SO_4}$ value of +6.6‰ (Fig. 6e) is still much closer to that of the original sulfate (+10.0‰) than to the −18‰ predicted if sulfide removal were exclusively due to NR-SOB activity (Fig. 4b). No contribution from NR-SOB results in constant $\delta^{18}O_{SO_4}$ values in these systems (Figs. 3c and 6b), whereas souring control exclusively due to NR-SOB would produce a 28‰ shift towards more negative $\delta^{18}O_{SO4}$ values (Fig. 4b). Therefore, the observed 3.4‰ shift in $\delta^{18}O_{SO_4}$ (+10.0‰ to +6.6‰; Fig. 6e) suggests that NR-SOB were only responsible for a fraction (12%) of the sulfide disappearance, which was still mainly due to biocompetitive exclusion (88%). Estimates of NR-SOB contributions based on $\delta^{18}O_{SO_4}$ values are plotted in Fig. 9 for both nitrate- and nitrite-treated bioreactors. This reveals a partial role for NR-SOB at low nitrite

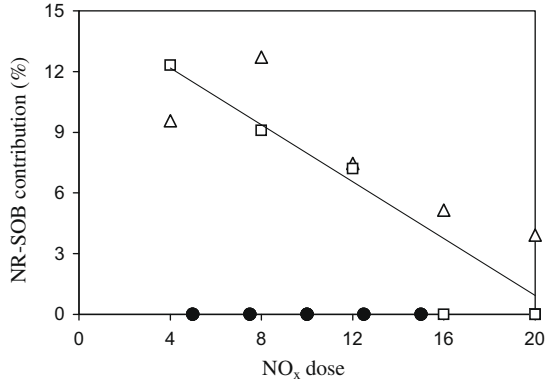

Fig. 9. Relative contribution from NR-SOB to the overall sulfide removal from the bioreactors as estimated by $\delta^{18}O_{SO_4}$ in relation to $mCSB_{SO_4}$ and $mCSB_{H_2O}$, as follows: NR-SOB contribution (%) = [(mean $\delta^{18}O_{mCSB-SO_4}$) − ($\delta^{18}O_{sample-SO_4}$)]/[(mean $\delta^{18}O_{mCSB-SO_4}$) − ($\delta^{18}O_{mCSB-H_2O}$)]. Calculations were performed for all $\delta^{18}O_{SO_4}$ data shown in Fig. 6b, and for the data shown in Fig. 6e that plot outside (below) standard deviations around the initial media values. Estimates are plotted as a function of NO_x dose for the bioreactor treated with nitrate (●) and bioreactors treated with nitrite (bioreactor A = △; bioreactor B = □). The regression line was calculated using NR-SOB contribution (%) estimates combined from both nitrite-treated bioreactors.

concentrations, whereas NR-SOB appear to play little to no role at high nitrite and all nitrate doses in these experiments.

4.4. Comparison of nitrate- and nitrite-treated bioreactors

Nitrate has one- to two-thirds more oxidation capacity than nitrite as an electron acceptor for NRB depending on whether nitrate or nitrite is reduced via denitrification to N_2 (transferring 5 or 3 electrons, respectively) or via dissimilatory nitrate or nitrite reduction to ammonia (transferring 8 or 6 electrons, respectively). Furthermore, the nitrate- and nitrite-treated experimental systems presented here differed even more with respect to the relative oxidation capacity of molar NO_x equivalents because the lactate concentration was higher in the nitrite-treated bioreactor experiments (Table 1). Both NRB-based souring control mechanisms in question ultimately depend on the depletion of organic electron donors (lactate) by these oxidants (Fig. 1 and Table 5; Hubert et al., 2003). Hence the smallest nitrite doses (4 and 8 mM) gave rise to relatively little sulfide removal (apparent $f \leqslant 0.35$; Fig. 5b), whereas the smallest nitrate doses, despite having even lower molarity (2.5 and 5 mM), were more effective at lowering the sulfide concentration (apparent $f \geqslant 0.55$; Fig 5a). Fig. 5c displays this difference by plotting apparent f values against molar NO_x doses applied to the bioreactors. It is possible that a different nitrate dosing regime that promoted lower apparent f may have allowed contributions from NR-SOB, as observed in the bioreactors that received low nitrite doses (Figs. 7 and 9). NR-SOB activity may thus be linked to overall redox conditions (e.g., high sulfide, low NO_x) rather than to using nitrite as the oxidant instead of nitrate.

5. CONCLUSIONS AND SIGNIFICANCE

The finding that biocompetitive exclusion took place in the nitrate-treated bioreactor confirms our earlier conclusions based on molecular community analyses and competitive co-culture physiology studies that lactate depletion by O-NRB occurred in this experimental system (Hubert and Voordouw, 2007). We previously speculated that NR-SOB were important microbial community members in the nitrite-treated bioreactors based on the persistence of low redox potential, SRB dominating molecular community profiles and SRB viable counts remaining high at the end of the experiments (Fig. 5; Hubert et al., 2005). The isotope results presented here confirm some NR-SOB activity at low nitrite doses, but also suggest that nitrite-reducing lactate-oxidizing O-NRB made the predominant contribution to the elimination of sulfide during nitrite treatment. NR-SOB may compete more successfully with O-NRB for NO_x electron acceptors in contexts where sulfide is more abundant, such as the low apparent f conditions in our experimental bioreactors (Figs. 6d and 9). However, any such advantage appears to diminish at lower sulfide concentrations (as apparent f approaches 1 due to higher NO_x doses; Fig. 8). Another explanation could be greater competitive fitness of these NR-SOB, relative to O-NRB, in the presence of low NO_x concentrations.

This study highlights the usefulness of sulfur and oxygen isotopes for distinguishing between organotrophic and lithotrophic nitrate or nitrite reduction pathways. Estimating relative contributions from these two processes using oxygen isotope ratios of sulfate may be particularly useful in settings where combinations of both NRB activities may be expected. Such diagnoses have industrial relevance, e.g., for oil production where management of reservoir souring depends on understanding the microbiology underpinning both the problem and the different solutions. Using oxygen isotope ratios of sulfate to understand natural biogeochemical cycling of elements other than sulfur has been reported previously (Ku et al., 1999). Our results indicate the potential for using $\delta^{18}O$ to understand nitrogen cycling in natural environments where nitrate or nitrite concentrations are relatively stable. Similarly in oil field settings, operators are more likely to introduce a single effective dose of nitrate into sour reservoirs, rather than experiment with different doses as in the laboratory tests presented here. Stable NO_x concentrations (in natural systems) or single NO_x dose scenarios (in oil fields) could preclude sulfur isotope-based determinations of nitrogen cycling in situations where isotope ratios for NR-SOB versus biocompetitive exclusion of SRB by O-NRB may be similar (Fig. 8). Assessing the influence of NR-SOB by determining $\delta^{18}O_{SO_4}$ values of sulfate (e.g., at injection and production wells relative to $\delta^{18}O_{H_2O}$ values in reservoir fluids) should, however, be possible.

Nitrate and nitrite treatment strategies for sour oil fields are becoming increasingly employed by oil companies worldwide. Knowledge of relative contributions from biocompetitive exclusion and sulfide oxidation to souring control regimes can offer valuable feedback for informed optimization and trouble shooting on a case-specific basis.

Stable isotope analyses, particularly oxygen isotope measurements as shown here, offer promise for advancing the current state of nitrate- and nitrite-based technology towards a better understanding of souring control by NRB and improved management of the oil field sulfur cycle.

ACKNOWLEDGMENTS

This work was supported by a Strategic Grant from the Natural Sciences and Engineering Research Council of Canada (NSERC) and by ConocoPhillips. C.H. was supported by NSERC, the Government of Alberta, the Alberta Ingenuity Fund, and the Max Planck Society. We thank Pat McCarron and Andrew Richardson from Petrovera Resources for providing water samples produced from the Coleville oil field. The authors wish to thank Benjamin Brunner, Michael Formolo and Wajih Naqvi for helpful discussions. We also thank Kevin Mandernack, Bill Gilhooly, an anonymous reviewer and Associate Editor Tim Lyons for constructive feedback that improved the article.

REFERENCES

Aharon P. and Fu B. (2000) Microbial sulfate reduction rates and sulfur and oxygen isotope fractionations at oil and gas seeps in deepwater Gulf of Mexico. *Geochim. Cosmochim. Acta* **64**, 233–246.

Aharon P. and Fu B. (2003) Sulfur and oxygen isotopes of coeval sulfate-sulfide in pore fluids of cold seep sediments with sharp redox gradients. *Chem. Geol.* **195**, 201–208.

APHA (American Public Health Association) (1992) *Standard Methods for the Examination of Water and Wastewater*. Washington, DC: American Water Works Association and Water Pollution Control Federation, pp. 439–440.

Balci N., Shanks, III, W. C., Mayer B. and Mandernack K. W. (2007) Oxygen and sulfur isotope systematics of sulfate produced by bacterial and abiotic oxidation of pyrite. *Geochim. Cosmochim. Acta* **71**, 3796–3811.

Bødtker G., Thorstenson T., Lillebø B. L. P., Thorbjørnsen B. E., Ulvøen R. H., Sunde E. and Torsvik T. (2008) The effect of long-term nitrate treatment on SRB activity, corrosion rate and bacterial community composition in offshore water injection systems. *J. Ind. Microbiol. Biotechnol.* **35**, 1625–1636.

Bolliger C., Schroth M. H., Bernasconi S. M., Kleikemper J. and Zeyer J. (2001) Sulfur isotope fractionation during microbial sulfate reduction by toluene-degrading bacteria. *Geochim. Cosmochim. Acta* **65**, 3289–3298.

Böttcher M. E., Thamdrup B. and Vennemann T. W. (2001) Oxygen and sulfur isotope isotope fractionation associated with bacterial disproportionation of elemental sulfur. *Geochim. Cosmochim. Acta* **65**, 1601–1609.

Brunner B., Bernasconi S. M., Kleikemper J. and Schroth M. H. (2005) A model for oxygen and sulfur isotope fractionation in sulfate during bacterial sulfate reduction processes. *Geochim. Cosmochim. Acta* **69**, 4773–4785.

Canfield D. E. (2001) Isotope fractionation by natural populations of sulfate-reducing bacteria. *Geochim. Cosmochim. Acta* **65**, 1117–1124.

Canfield D. E., Olesen C. A. and Cox R. P. (2006) Temperature and its control of isotope fractionation by a sulfate-reducing bacterium. *Geochim. Cosmochim. Acta* **70**, 548–561.

Chiba H. and Sakai H. (1985) Oxygen isotope exchange rate between dissolved sulfate and water at hydrothermal temperatures. *Geochim. Cosmochim. Acta* **49**, 993–1000.

Clark I. and Fritz P. (1997) *Environmental Isotopes in Hydrogeology*. Lewis Publishers, Boca Raton, New York, 328 pp.

Cord-Ruwisch R. A. (1985) A quick method for determination of dissolved and precipitated sulfides in cultures of sulfate reducing bacteria. *J. Microbiol. Methods* **4**, 33–36.

Dale A. W., Brüchert V., Alperin M. and Regnier P. (2009) An integrated sulfur isotope model for Namibian shelf sediments. *Geochim. Cosmochim. Acta* **73**, 1924–1944.

De Gusseme B., De Schryver P., De Cooman M., Verbeken K., Boeckx P., Verstraete W. and Boon N. (2009) Nitrate-reducing, sulfide-oxidizing bacteria as microbial oxidants for rapid biological sulfide removal. *FEMS Microbiol. Ecol.* **67**, 151–161.

Detmers J., Brüchert V., Habicht K. S. and Kuever J. (2001) Diversity of sulfur isotope fractionations by sulfate-reducing prokaryotes. *Appl. Environ. Microbiol.* **67**, 888–894.

Eckford R. E. and Fedorak P. M. (2002) Chemical and microbiological changes in laboratory incubations of nitrate amendment "sour" produced waters from three western Canadian oil fields. *J. Ind. Microbiol. Biotechnol.* **29**, 243–254.

Epstein S. and Mayeda T. (1953) Variations of ^{18}O content of waters from natural sources. *Geochim. Cosmochim. Acta* **4**, 213–224.

Ferguson P. R., Weinrauch N., Wassenaar L. I., Mayer B. and Veizer J. (2007) Isotope constraints on water, carbon, and heat fluxes from the northern Great Plains region of North America. *Global Biogeochem. Cycles*, 21, GB2023. doi:10.1029/2006GB002702.

Fritz P., Basharmal G. M., Drimmie R. J., Ibsen J. and Qureshi R. M. (1989) Oxygen isotope exchange between sulphate and water during bacterial reduction of sulphate. *Chem. Geol.* **79**, 99–105.

Fry B. (2006) S*table Isotope Ecology*. Springer Science + Business Media, LLC, New York, 308 pp.

Fry B., Cox J., Gest H. and Hayes J. M. (1986) Discrimination between ^{34}S and ^{32}S during bacterial metabolism of inorganic sulfur compounds. *J. Bacteriol.* **165**, 328–330.

Gevertz D., Telang A., Voordouw G. and Jenneman G. (2000) Isolation and characterization of strains CVO and FWKO B, two novel nitrate-reducing, sulfide oxidizing bacteria isolated from oil field brine. *Appl. Environ. Microbiol.* **66**, 2491–2501.

Greene E. A., Hubert C., Nemati M., Jenneman G. and Voordouw G. (2003) Nitrite reductase activity of sulfate-reducing bacteria prevents their inhibition by nitrate-reducing, sulfide-oxidizing bacteria. *Environ. Microbiol.* **5**, 607–617.

Greene E. A., Brunelle V., Jenneman G. E. and Voordouw G. (2006) Synergistic inhibition of microbial sulfide production by combinations of the metabolic inhibitor nitrite and biocides. *Appl. Environ. Microbiol.* **72**, 7897–7901.

Grigoryan A. A., Cornish S. L., Buziak B., Lin S., Cavallaro A., Arensdorf J. J. and Voordouw G. (2008) Competitive Oxidation of Volatile Fatty Acids by Sulfate- and Nitrate-Reducing Bacteria from an Oil Field in Argentina. *Appl. Environ. Microbiol.* **74**, 4324–4335.

Harrison A. G. and Thode H. G. (1957) The kinetic isotope effect in the chemical reduction of sulphate. *Trans. Faraday Soc.* **54**, 84–92.

Harrison A. G. and Thode H. G. (1958) Mechanisms of bacterial reduction of sulphate from isotope fractionation studies. *Trans. Faraday Soc.* **54**, 84–92.

Haveman S. A., Greene E. A., Stilwell C. P., Voordouw J. K. and Voordouw G. (2004) Physiological and gene expression analysis of inhibition of *Desulfovibrio vulgaris* Hildenborough by nitrite. *J. Bacteriol.* **186**, 7944–7950.

Hubert C. and Voordouw G. (2007) Oil field souring control by nitrate-reducing *Sulfurospirillum* spp. that outcompete sulfate-

reducing bacteria for organic electron donors. *Appl. Environ. Microbiol.* **73**, 2644–2652.

Hubert C., Nemati M., Jenneman G. and Voordouw G. (2005) Corrosion risk associated with microbial souring control using nitrate or nitrite. *Appl. Microbiol. Biotechnol.* **68**, 272–282.

Hubert C., Nemati M., Jenneman G. and Voordouw G. (2003) Containment of biogenic sulfide production in continuous up-flow packed-bed bioreactors with nitrate or nitrite. *Biotech. Prog.* **19**, 338–345.

Jørgensen B. B. (2006) Bacteria and marine biogeochemistry. In *Marine Geochemistry* (eds. H. D. Schulz and M. Zabel). Springer, Berlin, Germany, pp. 169–206.

Jurelevicius D., von der Weid I., Korenblum E., Valoni E., Penna M. and Seldin L. (2008) Effect of nitrate injection on the bacterial community in a water–oil tank system analyzed by PCR-DGGE. *J. Ind. Microbiol. Biotechnol.* **35**, 251–255.

Kaplan I. R. and Rittenberg S. C. (1964) Microbiological fractionation of sulphur isotopes. *J. Gen. Microbiol.* **34**, 195–212.

Kjellerup B. V., Veeh R. H., Sumithraratne P., Thomsen T. R., Buckingham-Meyer K., Frølund B. and Sturman P. (2005) Monitoring of microbial souring in chemically treated, produced-water biofilm systems using molecular techniques. *Appl. Microbiol. Biotechnol.* **32**, 163–170.

Knoeller K., Vogt C., Richnow H. and Weise S. (2006) Sulfur and oxygen isotope fractionation during benzene, toluene, ethyl benzene and xylene degradation by sulfate-reducing bacteria. *Environ. Sci. Technol.* **40**, 3879–3885.

Ku T. C. W., Walter L. M., Coleman M. L., Blake R. E. and Martini A. M. (1999) Coupling between sulfur recycling and syndepositional carbonate dissolution: evidence from oxygen and sulfur isotope composition of pore water sulfate, South Florida Platform, USA. *Geochim. Cosmochim. Acta* **63**, 2529–2546.

Lloyd R. M. (1967) Oxygen-18 composition of oceanic sulfate. *Science* **156**, 1228–1231.

Mangalo M., Meckenstock R. U., Stichler W. and Einsiedl F. (2007) Stable isotope fractionation during bacterial sulfate reduction is controlled by reoxidation of intermediates. *Geochim. Cosmochim. Acta* **71**, 4161–4171.

Mangalo M., Einsiedl F., Meckenstock R. U. and Stichler W. (2008) Influence of the enzyme dissimilatory sulfite reductase on stable isotope fractionation during sulfate reduction. *Geochim. Cosmochim. Acta* **72**, 1513–1520.

Mizutani Y. and Rafter T. A. (1969) Oxygen isotopic composition of sulphates: Part 4. Bacterial fractionation of oxygen isotopes in reduction of sulphate and in the oxidation of sulphur. *N. Z. J. Sci.* **12**, 60–68.

Mizutani Y. and Rafter T. A. (1973) Isotopic behaviour of sulphate oxygen in the bacterial reduction of sulphate. *Geochem. J.* **6**, 183–191.

Naqvi S. W. A., Jayakumar D. A., Narvekar P. V., Naik H., Sarma V. V. S. S., D'Souza W., Joseph S. and George M. D. (2000) Increased marine production of N_2O due to intensifying anoxia on the Indian continental shelf. *Nature* **408**, 346–349.

Nemati M., Mazutinec T., Jenneman G. and Voordouw G. (2001) Control of biogenic H_2S production by nitrite and molybdate. *J. Ind. Microbiol. Biotechnol.* **26**, 350–355.

Peng H., Mayer B., Harris S. and Krouse H. R. (2004) A 10-year record of stable isotope compositions of hydrogen and oxygen in precipitation at Calgary, Alberta, Canada. *Tellus B.* **56**, 147–159.

Rees C. E. (1973) A steady-state model for sulphur isotope fractionation in bacterial reduction processes. *Geochim. Cosmochim. Acta* **37**, 1141–1162.

Schwermer C. U., Lavik G., Abed R. M. M., Dunsmore B., Ferdelman T. G., Stoodley P., Gieseke A. and de Beer D. (2008) Impact of nitrate on the structure and function of bacterial biofilm communities in pipelines used for injection of seawater into oil fields. *Appl. Environ. Microbiol.* **74**, 2841–2851.

Spence M. J., Bottrell S. H., Thorton S. F. and Lerner D. N. (2001) Isotopic modelling of the significance of bacterial sulphate reduction for Phenol attenuation in a contaminated aquifer. *J. Contam. Hydrol.* **53**(3–4), 285–304.

Strebel O., Böttcher J. and Fritz P. (1990) Use of isotope fractionation of sulfate–sulfur and sulfate–oxygen to assess bacterial desulfurication in a sandy aquifer. *J. Hydrol.* **121**, 155–172.

Taylor B. E. and Wheeler M. C. (1994) Sulfur- and oxygen-isotope geochemistry of acid mine drainage in the Western United States: field and experimental studies revisited. In *Environmental Geochemistry of Sulfide Oxidation* (eds. C. N. Alpers and D. W. Blowes). ACS Symposium Series. Amer. Chem. Soc, Washington, DC, pp. 481–514.

Telang A. J., Ebert S., Foght J. M., Westlake D. W. S., Jenneman G. E., Gevertz D. and Voordouw G. (1997) The effect of nitrate injection on the microbial community in an oil field as monitored by reverse sample genome probing. *Appl. Environ. Microbiol.* **63**, 1785–1793.

Telang A. J., Jenneman G. E. and Voordouw G. (1999) Sulfur cycling in mixed cultures of sulfide-oxidizing and sulfate- or sulfur-reducing oil field bacteria. *Can. J. Microbiol.* **45**, 905–913.

Van Stempvoort D. R. and Krouse H. R. (1994) Controls of $\delta^{18}O$ in sulfate: review of experimental data and application to specific environments. In *Environmental Geochemistry of Sulfide Oxidation* (eds. C. N. Alpers and D. W. Blowes). ACS Symposium Series. Amer. Chem. Soc, Washington, DC, pp. 446–480.

Voordouw G., Voordouw J. K., Jack T. R., Foght J., Fedorak P. M. and Westlake D. W. S. (1992) Identification of distinct communities of sulfate-reducing bacteria in oil fields by reverse sample genome probing. *Appl. Environ. Microbiol.* **58**, 3542–3552.

Voordouw G., Armstrong S. M., Reimer M. F., Fouts B., Telang A. J., Shen Y. and Gevertz D. (1996) Characterization of 16S rRNA genes from oil field microbial communities indicates the presence of a variety of sulfate-reducing, fermentative, and sulfide-oxidizing bacteria. *Appl. Environ. Microbiol.* **62**, 1623–1629.

Wortmann U. G., Chernyavsky B., Bernasconi S. M., Brunner B., Böttcher M. E. and Swart P. K. (2007) Oxygen isotope biogeochemistry of pore water sulfate in the deep biosphere: dominance of isotope exchange reactions with ambient water during microbial sulfate reduction (ODP Site 1130). *Geochim. Cosmochim. Acta* **71**, 4221–4232.

Zak I., Sakai H. and Kaplan I. R. (1980) Factors controlling the $^{18}O/^{16}O$ and $^{34}S/^{32}S$ isotope ratios of ocean sulfates, evaporates and interstitial sulfates from modern deep sea sediments. In *Isotope Marine Chemistry* (eds. E. D. Goldberg, Y. Horibe and K. Saruhaski). Rokakuho, Tokyo, pp. 339–373.

Zerkle A. J., Farquhar J., Johnston D. T., Cox R. P. and Canfield D. E. (2009) Fractionation of multiple sulfur isotopes during phototrophic oxidation of sulfide and elemental sulfur by a green sulfur bacterium. *Geochim. Cosmochim. Acta* **73**, 291–306.

Zopfi J., Böttcher M. E. and Jørgensen B. B. (2008) Biogeochemistry of sulfur and iron in *Thioploca*-colonized surface sediments in the upwelling area off central Chile. *Geochim. Cosmochim. Acta* **72**, 827–843.

Associate editor: Tim Lyons